

PREDICTIVE VARIABLES OF COUNTER-SHOCK DURING RESUSCITATION IN
A SWINE MODEL

By

Daniel N. Allen

A Thesis Submitted to the Faculty of the
GRADUATE INTERDISCIPLINARY PROGRAM OF BIOMEDICAL ENGINEERING
In Partial Fulfillment of the Requirements for the Degree of
MASTER OF SCIENCE WITH A MAJOR IN BIOMEDICAL ENGINEERING
In the Graduate College
THE UNIVERSITY OF ARIZONA

2010

STATEMENT BY AUTHOR

This thesis has been submitted in partial fulfillment of requirements for an advanced degree at The University of Arizona and is deposited in the University Library to be made available to borrowers under rules of the Library.

Brief quotations from this thesis are allowable without special permission, provided that accurate acknowledgment of source is made. Requests for permission for extended quotation from or reproduction of this manuscript in whole or in part may be granted by the head of the major department or the Dean of the Graduate College when in his or her judgment the proposed use of the material is in the interests of scholarship. In all other instances, however, permission must be obtained from the author.

SIGNED: Daniel N. Allen

APPROVAL BY THESIS DIRECTOR

This thesis has been approved on the date shown below :

Julia H. Indik
Julia H. Indik
Associate Professor of Medicine

December 17, 2010
Date

TABLE OF CONTENTS

LIST OF FIGURES.....	5
LIST OF TABLES.....	7
ABSTRACT.....	8
INTRODUCTION.....	9
Ventricular Fibrillation.....	11
Defibrillation.....	13
History of CPR.....	16
Resuscitation Methods.....	21
Swine Model.....	21
Resuscitation Variables.....	22
<i>Coronary Perfusion Pressure</i>	23
<i>End-Tidal CO₂ (ET-CO₂)</i>	25
<i>Amplitude Spectral Area (AMSA)</i>	26
<i>Slope</i>	27
<i>Myocardial Infarct</i>	28
<i>Duration of Untreated VF</i>	28
Purpose.....	29
Overview of the Study.....	29
METHODS.....	32
Induction of Anesthesia.....	32
Ventilation and Maintaining Sedation.....	33
Instrumentation.....	33
Plug Placement.....	34
Resuscitation.....	34
Data Calculation.....	36
<i>AMSA and Slope</i>	37
<i>ET-CO₂</i>	38
<i>CPP</i>	38
Statistical Analysis.....	41
RESULTS.....	42
2 nd and Higher Shocks – Univariate Analysis.....	42
<i>CPP Variables</i>	43
<i>CO₂ Variables</i>	49
<i>ECG Waveform Variables</i>	51

TABLE OF CONTENTS - Continued

<i>Binary Variables</i>	54
2 nd and Higher Shocks – Multivariate Analysis.....	55
All Shocks – Univariate Analysis.....	55
<i>ECG Waveform Variables</i>	56
<i>Binary Variables</i>	56
All Shocks – Multivariate Analysis.....	57
Sensitivity and Specificity Analysis.....	58
DISCUSSION.....	62
Limitations.....	64
Future Work.....	65
Conclusion.....	65
REFERENCES.....	67

LIST OF FIGURES

FIGURE 1.	Comparison of normal and ventricular fibrillation ECG waveforms	12
FIGURE 2.	A cross section view of the human heart, with electrophysiological anatomy exposed	13
FIGURE 3.	A visual representation depicting charge and current differences between monophasic and biphasic shocks	14
FIGURE 4.	Graphical representation of CPP calculation - the difference between diastolic phase aortic and right atrial pressures	24
FIGURE 5.	Flowchart of resuscitation protocol	37
FIGURE 6.	Graphical representation for final end-diastole CPP calculation	39
FIGURE 7.	Graphical representation of mean end-diastole CPP calculation	39
FIGURE 8.	Graphical representation of mean end-diastole CPP integration	40
FIGURE 9.	Final CPP vs Mean CPP	46
FIGURE 10.	MDI CPP vs Mean CPP	46
FIGURE 11.	Box-Whisker Plot of Final CPP	47
FIGURE 12.	Box-Whisker Plot of Mean CPP	48
FIGURE 13.	Box-Whisker Plot of MDI CPP	48
FIGURE 14.	Box-whisker plot of Final CO ₂	50
FIGURE 15.	Box-whisker plot of Mean CO ₂	51
FIGURE 16.	Slope vs AMSA	52
FIGURE 17.	Box-whisker plot of Slope	53
FIGURE 18.	Box-whisker plot of AMSA	54

LIST OF FIGURES - Continued

FIGURE 19. Sensitivity and specificity as a function of slope, created from 1 st shock excluded data	60
FIGURE 20. Sensitivity and specificity as a function of AMSA, created from 1 st shock excluded data	60
FIGURE 21. Sensitivity and specificity as a function of Slope, created from data including all shocks	61
FIGURE 22. Sensitivity and specificity as a function of AMSA, created from data including all shocks	61

LIST OF TABLES

TABLE 1.	Baseline Populations and Hemodynamics	43
TABLE 2.	Tertile Divisions of variables and their description (Duration of VF and MI variables were not applicable for tertiles)	44
TABLE 3.	Spearman rank coefficients for CPP variables	45
TABLE 4.	Summary of CPP variables as predictors for successful counter-shock	45
TABLE 5.	Spearman rank coefficients for CO2 variables	49
TABLE 6.	Summary of CO2 variables as predictors for successful counter-shock	49
TABLE 7.	Spearman rank coefficient for ECG variables	52
TABLE 8.	Summary of ECG waveform variables as predictors of successful counter-shock	53
TABLE 9.	Summary of binary variables as predictors for successful counter-shock	55
TABLE 10.	Tertile values for AMSA and slope in the “all shocks” population	56
TABLE 11.	Results of the univariate logistic regression for AMSA and slope for the extended population of shocks	56
TABLE 12.	Results of the univariate logistic regression for MI and duration of VF for the extended population of shocks	57
TABLE 13.	Summary of multivariate logistic regression of AMSA, slope, MI, and duration of VF	58
TABLE 14.	Areas under the curves for sensitivity/specificity analysis of AMSA and slope	59

ABSTRACT

The purpose of this study was to examine parameters with potential to predict the outcome of counter-shocks during resuscitation. Out-of-hospital discharge rates decline 8-10% per minute of untreated cardiac arrest (3,4), therefore time wasted during resuscitation for unsuccessful counter-shocks can be reduced if scrutiny is given toward additional variables of predictive ability.

Our experiment was designed to find the predictive ability of amplitude spectral area (AMSA), slope, end-tidal carbon dioxide, coronary perfusion pressure, the condition of acute myocardial infarction (MI), and the duration of ventricular fibrillation (VF) induced cardiac arrest preceding resuscitation in a swine model. Variables were tested by logistic regression ($\alpha = 0.1$). Groups were set up in a 2x2 design: MI versus control; 2 minute vs 8 minute VF.

We found AMSA, slope, MI and duration of VF significant predictors of counter-shock. We also found AMSA, slope, and duration of VF as independent predictors of counter-shock.

INTRODUCTION

Cardiovascular disease is the number one fatal disease in the country. This disease includes heart disease, stroke, hypertension, and other diseases of the arteries. In 2006, there were approximately 800,000 deaths related to cardiovascular disease, a significant decline since the million deaths in 1985. Additionally, hospital discharges of cardiovascular disease related admissions was up to 6 million in 2006 (from 5 million in 1985) suggesting an improvement of intervention over the past 25 years (1). Another important statistic to review is heart disease. In 2006, the leading cause of death in the country was heart disease at 631,636 deaths. Of these deaths, coronary heart disease accounted for 68% of them (2).

Furthermore, the prevalence of heart failure in the United States was approximated at well over a million in 2006 (2). However, over the past 25 years, heart failure related deaths have been dramatically reduced. Reported heart failure related deaths in 1985 were nearly 800,000, arguably a victory of the fitness and antidrug campaigning of the 1990s and this decade. On the other hand, recent surges of incidence and prevalence of adolescent and adult obesity and type 2 diabetes are cause to be concerned. As potential causes of heart failure, diabetes and obesity prevalence have been on the rise for the last 50 years. For example, obesity in adults was 10.1% in males in 1960 whereas today the statistic is 33.1% (1). Similar comparisons can be made with type 2 diabetes prevalence in adolescents and adults. Therefore, although heart failure related

deaths are declining, a younger and unhealthier generation will only buff the statistic in the future, and making efforts now for prevention and intervention more significant. Our study focuses on intervention through the scope of resuscitation. In the end, we hope our efforts may contribute to a continued decline in cardiovascular and heart related deaths in the future.

It is the goal of the Sarver Heart Center at the University of Arizona to reduce the mortality rate from heart disease by researching better methods of resuscitation and emergency healthcare. At this location, I have worked as a research specialist under the mentorship of Dr. Julia H. Indik since June 2007, with hopes to increase the efficiency of resuscitation by exploring predictive variables of successful counter-shocks. This document represents the collection of observations, analysis, and work put in over the last 3 years to increase the survival rate, particularly in ventricular fibrillation related cases of heart failure and is intended to fulfill the thesis and research requirements of the University of Arizona Graduate School of Biomedical Engineering.

The paper is divided into four main sections: Introduction, Methods, Results, and Discussion. The remainder of the introduction will review important terms and concepts relevant to current research in cardiopulmonary resuscitation. Specifically, these concepts are ventricular fibrillation, defibrillation, history of CPR, resuscitation methods, swine model, resuscitation variables, and overview of the study.

Ventricular Fibrillation

The cardio-pulmonary system of the body is responsible for delivering oxygen and nutrients to cells as well as carrying metabolites and carbon dioxide away from the cells. When the circulatory system is compromised, metabolites build up in the blood and cells are deprived of oxygen and important nutrients. If poor circulation continues, the tissue dies. In cases involving coronary heart disease, the heart tissue becomes necrotic and scarring process results. The myocardium is scarred in regions with the myocardial infarction, or occlusion of a coronary artery. The heart is left in a weakened state which can include a decline of cardiac output, ejection fraction, and contractility. If the region of tissue death is large enough, the heart can no longer sustain the patient's lifestyle, or may even be fatal through heart failure. Prolonged periods of hypotension, hypoxia/ischemia, or cardiac-arrhythmia, infarct, and other non-ischemic causes may result in heart failure. The worst manifestation of heart failure is a well-known cardiac-arrhythmia: Ventricular Fibrillation (VF).

VF is diagnosed by electrocardiogram depicting disorganized electrical activity. The characteristic QRS complex of a healthy rhythm is replaced by disorganized and erratic ventricular depolarization. Normal electrical conduction in the heart travels from the sinoatrial node to the atrioventricular node, then to the bundle of His and onto the Purkinje fibers (figure 2). The net effect is a ventricular contraction originating at the apex which spreads upwards, forcing blood through the aortic valve. During VF, the electrical signal is entirely disorganized such that there is no organized mechanical

contraction and therefore the ventricle cannot generate a pressure. Circulation is arrested (“cardiac arrest”) and the patient loses physical autonomy as well as cognizance. A previous study has shown an 8-10% loss in likelihood of hospital discharge for every minute elapsed during cardiac arrest (3, 4). And without quick and efficient response along with defibrillation, the patient would never recover.

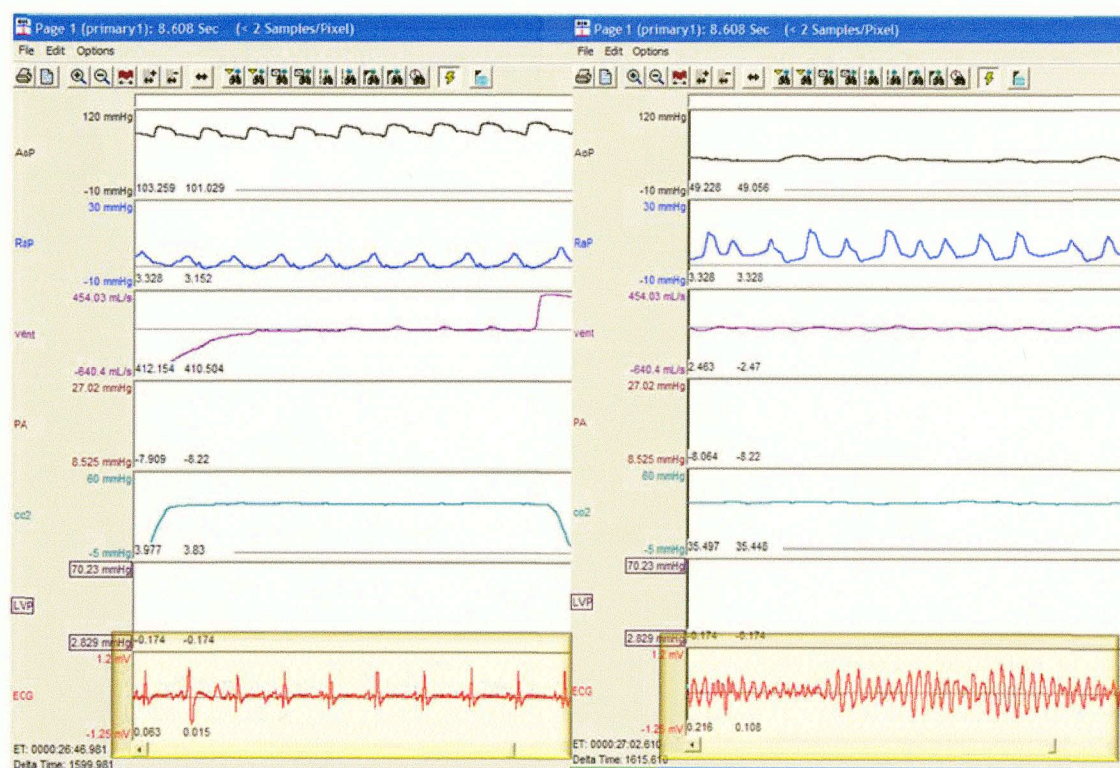


FIGURE 1: Comparison of normal and ventricular fibrillation ECG waveforms.

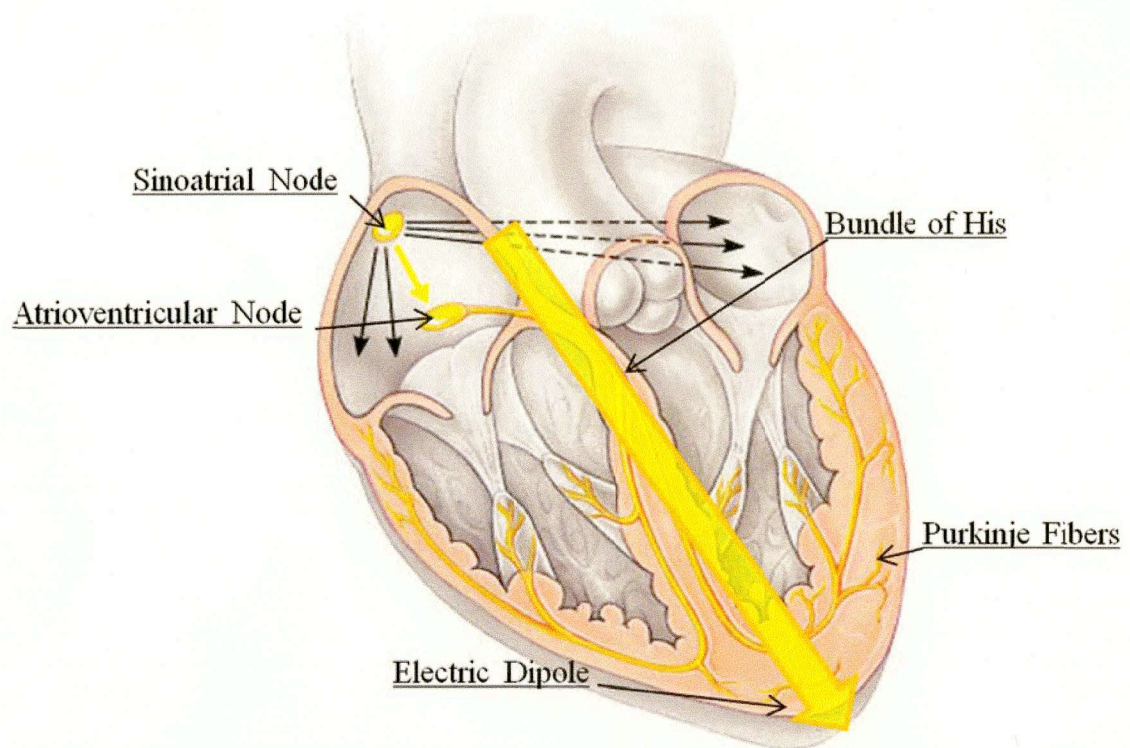


FIGURE 2: A cross section view of the human heart, with electrophysiological anatomy exposed.

Defibrillation

In 1899, two physicists from the University of Geneva demonstrated that VF could be reversed in dogs when a large voltage was placed across the heart. Almost fifty years later, Claude Beck, professor of surgery at Case Western University, was the first to demonstrate defibrillation in humans by the same technique, while performing open heart surgery on a 14 year old boy (5). Today, emergency response teams carry automated external defibrillators (AED) with them in case the victims they come in contact with suffer from VF or other serious arrhythmias.

Current defibrillators provide either a monophasic or biphasic current across two separate leads stuck to the patient's chest, arranged to deliver depolarization of myocardial cells down the electrical dipole of the heart. The monophasic model has been outdated by a biphasic model. The rationale is that during a VF counter-shock, not all the myocytes can be depolarized by a single phasic shock. Some myocytes hyperpolarize while the rest depolarize. Furthermore, myocytes closest to the electrodes receive too much energy while the myocytes furthest away receive too little energy. However, a bipolar shock counters both problems by sending a biphasic charge allowing myocytes and allowing depolarization of all the myocytes at some point during the shock. The biphasic defibrillator has been demonstrated as superior in the field (6). Figure 3 provides a graphical representation for a biphasic shock.

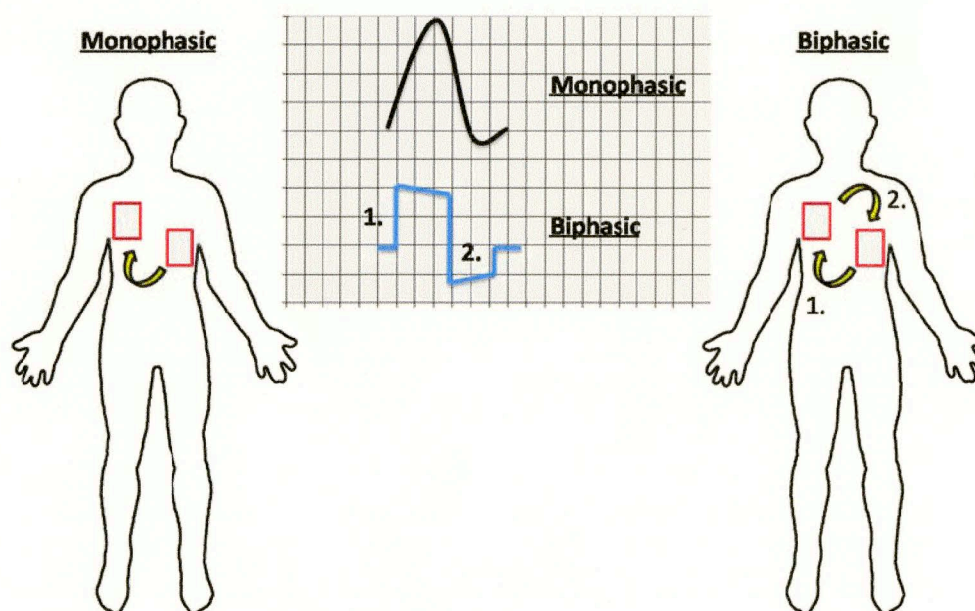


FIGURE 3: A visual representation depicting charge and current differences between monophasic and biphasic shocks.

There has been debate regarding the amount of energy necessary to defibrillate the heart. Although extreme voltage provides complete depolarization, superfluous amounts of power cause irreversible myocardial damage (7-14). The myocardial injury is then exacerbated by reduced cardiac output following resuscitation, potentially increasing post-reperfusion injury.

External defibrillators use high level voltages in order to overcome the high resistance of the skin. Depending on the assessed resistance of the patient by the defibrillator, the counter shock supplied can be from 150-300 Joules. Lower energy settings are preferred over higher settings in order to limit damage. Additionally, limiting the number of shocks during resuscitation is preferred over applying stacked shocks to reduce damage to the myocardium as well as to reduce the time without chest compressions during resuscitation (15).

In conclusion, the preferred treatment for VF is a counter-shock, aligned with the dipole of the heart, given by an external defibrillator. To increase the survival rate of VF victims, professionals select the manufacturer's suggested energy setting (if unknown, the setting is defaulted to 200J) and time the counter-shocks to be given during resuscitation at optimal moments for a favorable probability of return of spontaneous circulation (ROSC). In order to facilitate bystander and quick response team resuscitation, automated versions of external defibrillators (AED) were created. An AED greatly simplifies resuscitation protocol by directing emergency responders when to compress the chest, ventilate, and counter-shock.

History of CPR

Cardio-pulmonary resuscitation has its earliest roots as far back as 3000 BC.

Anthropologists have found Mayan and Incan hieroglyphics in cave drawings and suggest their meaning as representations of rectal fumigation, a process in which hot air is directed through the patient's rectum (16). This method is consistent with early theories of medical treatment. The mainstay treatment for the apparently "dead" was warmth and stimulation (16). The main objective for treatment of the victim was to return elements of "life" to lifelessness. Coldness would be treated by penetrating heat and stillness by touch, thereby restoring balance.

Other primitive and early methods for resuscitation involved derivations for providing warmth and stimulation. In order to put off death, the patient was smothered or bathed in warm ashes, burning excrement, and hot water (17). Methods of stimulation included flagellation (whipping or slapping) and odiferous salts and minerals placed near the patient's nose (17).

It is likely primitive resuscitation methods evolved to include more sophisticated tools and methods. Beginning in the 1500s, treatments utilized bellows from a furnace to blow hot air and smoke into the victim's mouth, an early predecessor for ventilation. This practice was continued until 1829 when a scientist at the Paris Academy of Science, Leroy d'Etiolles, demonstrated over distension of the lungs could be fatal in animals (17).

Instruments for rectal fumigation were also developed by native Americans in the 1700s. The responder would blow tobacco smoke into a bellows created from an animal

bladder. The outlet was inserted into the patients rectum and the smoke was pumped inside (16). The introduction of tobacco to the treatment is a significant development from Myan and Incan use 4700 years earlier because of the medicinal qualities of the plant. Tobacco leaves were well known for removing moisture and providing warmth. Tobacco fumigation techniques were taught to European colonists during the 1700s and were introduced in England in 1767. Fumigation continued to be practiced until British physiologist Benjamin Brodie demonstrated lethal doses of tobacco to cats and dogs in 1811 (17).

With increases of maritime activity, sudden death from drowning was becoming more common. One result was the popular acceptance of an ancient Egyptian treatment called “inversion.” The patient was hung by the ankles with chest and airway below the legs, allowing chest pressure to aid in expiration and pressure release to aid in inspiration (17). The other development was the creation of humane organizations with intent to respond to drown cases. One of the first organized was the Society for the Recovery of Drowned Persons in Amsterdam in 1767 (16). Other organizations were established soon after throughout Europe: Venice, Hamburg, Milan, St. Petersburg, Vienna, Paris, and London. Each organization had specific guidelines for responders to follow. The example below is taken from the Dutch Society for Recovery of Drowned Persons (17).

- Warm the Victim (By close proximity to fire, physical contact with volunteers, warm bath, or burying in warm sand)

- Remove swallowed or aspirated water (By lowering upper torso below the lower torso and applying manual pressure to the abdomen)
- Stimulate the victim (by rectal fumigation with tobacco smoke or the use of smelling salts under the nose)
- Restore breathing (By artificial breathing with a bellows)
- Bloodletting

Skepticism began to penetrate the time honored methods of resuscitation in the late 1700s, begging the development of better methods. In 1773, rescuers were taught to hoist the victim onto a wine barrel to be rolled back and forth (17). The result of this technique was compression of the chest as well as artificial ventilation. Defibrillation by electric shock was first suggest by Goodwin and Kite in 1778, largely in response for their reasoning that cardiac arrest was due to asphyxia. Emergency responders in Russia began burying victims in thin layers of snow and ice in 1803, in order to reduce the body's metabolism (17). This technique goes far to represent a shift in medical theory based upon restoring balance through warmth. In 1812, lifeguards of the humane societies were equipped with horses in order to hoist the victim into the saddle and set the horse on a trot down the beach (17). Similar to the wine barrel method, chest compression and artificial ventilation was a result.

Then came the medical revolution, deeply entrenched in the industrial revolution. With the onset of anesthesia, there was an increase of victims in respiratory arrest. The 1850s brought two novel methods for resuscitation. The first was mouth to mouth

ventilation. The second was the shift in priority from warming the victim to providing ventilation, un-occluded by the tongue falling back into the airway. Marshall Hall challenged the guidelines of the Royal Humane Society, suggesting precious time was lost transporting the victim and injury was further compounded by without some type of ventilation (17). Ventilation by bellows had been banned in 1829 in fear of over distension of the lungs. In 1856 Marshall developed a new method which incorporated artificial ventilation by rolling the victim back and forth from side to the prone position, 16 times per minute. When the patient was in the prone phase of the cycle, a compression was given to the victim's back.

Marshall's method was modified further in 1858. Instead of rolling the victim, the arms would be raised to the head with the patient in the supine position, followed by moving the arms downward forcefully to the patient's sides at 16 cycles per minute. Physicians solved the tongue in the airway blockage notorious for supine resuscitation by turning the victims head to the side. This technique was dubbed Sylvester's Method (17).

With priority taken away from moving the victim to warmth, the 1890s also saw innovation to resuscitation methodology. Dr. Friedrich Maass began pushing the societies to adapt chest compression cycles in 1891. French physicians began exploring additional methods for improving ventilation efficacy by stretching the patient's tongue rhythmically during resuscitation (17).

Innovations for resuscitation in the 1900s came much quicker. The Sylvester method was changed by physicians Holger and Neilson in 1932. They supported

resuscitation in the prone position with cyclic compressions on the back followed by lifting the elbows to allow inhalation (17). This new method was well publicized. Exposure went as far as to be included into the Boy Scout Handbook and established as military guidelines for resuscitation. Additional changes to resuscitation included the development of defibrillation at Case Western Reserve University in 1947, and the adoption of mouth to mouth ventilation in 1956.

One of the greatest contributions to resuscitation technique was made by Dr. William Kouwenhoven, an electrical/biomedical engineer, in 1960. Kouwenhoven is credited for developing the closed chest massage, contemporarily known as the modern chest compression. He argued for the necessity to maintain sufficient oxygen transport to the brain during cardiac arrest, even through minimal blood circulation (17). The American Heart Association and several International organizations adopted the new found method and programs were initiated to educate physician, soldier, and citizen. In 1972, Leonard Cobb hosted the world's first mass citizen training to an audience over 100,000. Publicity thereafter accelerated to the programs in place today.

Publicity for modern resuscitation methods in the United States, and arguably the world, are lead today by the American Heart Association and Red Cross. Resuscitation methods have become much more sophisticated with the advance of emergency medicine research and technology. As a result, methods have become more specific (methods of optimal CPR vary by cause of cardiac arrest, patient type, responder type, and instruments available). CPR methods will continue to become more sophisticated and

efficient as scientists and physicians continue their research, like those at the Sarver Heart Center at my location of study.

Resuscitation Methods

Advanced cardiac life support (ACLS) is a complex set of guidelines and priorities of treatments during resuscitation. To optimize the rate of survival of cardiac arrest, response teams utilize chest compressions, ventilation, counter-shocks, and pharmaceuticals to increase oxygen saturation of peripheral blood (SPO₂), circulate blood to the heart/lungs and head, restore a perfusing rhythm, and stabilize vitals post resuscitation. Although ACLS methods are formulaic, they can ultimately be tailored by a trained professional to adapt toward the patient's needs.

At the Sarver Heart Center, we use a swine model for our research. Our resuscitation method is a pre-specified resuscitation protocol derived from ACLS guidelines. Specific description of the resuscitation protocol is outlined in the methods section.

Swine Model

There are many advantages for the use of swine for experimental resuscitation studies. First, humans and swine have similar internal anatomical structures and neonatal development. This makes swine useful models in studying immunology, anesthesiology, neonatology, interventional radiology, renal failure, pharmacology, wound healing, and cardiothoracic interventions (18). Swine and human vasculature also share similar

material properties. Levels of collagen, fibrin and elastin proteins are near identical in the aortic root, and therefore human principles of blood vessel fluid dynamics and elasticity are observed in swine (18).

Along with anatomical and material similarities, swine models provide a middle ground for models. At the lower threshold, mouse and rat models serve biomedical research demands economically, being able to test large populations under constrained time demands in very controlled groups. The other end of the spectrum is the chimpanzee model. Humans and chimpanzees share more anatomical, neonatal, and material features than any other species. However, research on chimpanzees is often laborious, checkered with safety hazards and incomparably more expensive. Swine provide a compromise. Despite the recent epidemic of H1N1 Influenza in 2009, there are still very few transmissible diseases between humans and pigs, and the swine model is considered low risk (18).

Swine do not provide a perfect solution for resuscitation studies. The skeletal-muscular structure is very different from that of humans. Chest-compression technique must be adapted between the two models (18). Although these cause significant concerns, there are too many benefits from a porcine model to dismiss it.

Resuscitation Variables

Knowing the ideal moment to counter-shock VF is difficult at best. However, outcomes can be improved by coupling counter-shock protocol to probability models and setting thresholds of acceptable error. Ideally, the number of shocks would be

minimized, thereby limiting post-resuscitation myocardial dysfunction and wasted seconds during CPR. Additionally, the hands-free duration during ECG analysis would also be limited, thus maximizing efficiency of treatment. Therefore, if there were a model that could predict the outcome of counter-shock, it would be of benefit to emergency responders. To create the model, significant variables must be shown as predictors for successful counter-shocks. The variables under review by this study are the following:

- Coronary Perfusion Pressure (CPP)
- End-Tidal CO₂ (ET-CO₂)
- Amplitude Spectral Area (AMSA)
- Slope
- Myocardial Infarct
- Duration of Untreated VF

This sub-section will review each variable in successive order.

Coronary Perfusion Pressure

Coronary perfusion pressure is defined as the difference between aortic and right atrial diastolic pressures (See figure 4). The variable serves as a valuable indicator for the quality of perfusion of the myocardium. Circulation to the heart enters the left and right coronary arteries through the aorta. Blood carried within the coronaries ultimately travel through microscopic vessels which make up the microcirculation of the heart. Eventually blood flow is pooled into the great cardiac vein and dumped into the right atrium. A

positive differential between aortic and right atrial pressures ensures oxygenated blood to flow to the heart muscle and is essential for life.

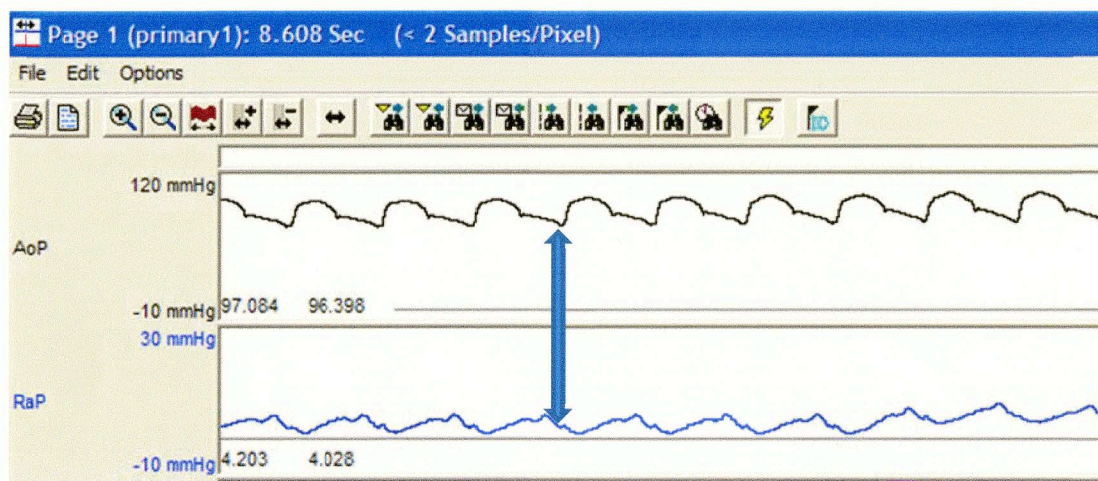


FIGURE 4: Graphical representation of CPP calculation - CPP is calculated by taking the difference between diastolic phase aortic and right atrial pressures.

During cardiac arrest, the low pressure and highly distensible portion of the heart and lungs fills with blood. Right atrial pressure steadily rises during arrest and becomes much greater than aortic pressure. The result is a negative coronary perfusion pressure, which must be overcome through chest compressions in CPR (19-21). If CPP remains negative, oxygenated blood cannot be delivered to the myocardium. Cardiac cells continue to hibernate and remain dormant until positive CPP can be restored. Negative CPP values can be overcome through resuscitation. Vasoconstrictors and chest compressions clear the pressure in right circulatory path and elevate aortic pressure. Oxygenated blood pulses through the coronary blood vessels once more and myocyte function is restored.

Coronary perfusion pressure is an invasive variable. Current methods for ascertaining CPP require cannulating major blood vessels of the body and placing transducers under fluoroscopy. One transducer is placed in the aorta and the other is passed through the pulmonary valve and into the right atrium. CPP acquisition, therefore, would be unrealistic for emergency responders to acquire in out-of-hospital arrests, and laborious in any environment. However, the variable has been shown to be a significant predictor of ROSC (22-25). A human study of cardiac arrest showed 79% of cardiac arrest victims achieved ROSC post resuscitation with CPP values greater than 25 mmHg (22). Perfusion pressure is important, and our study will observe its capacity to predict the immediate outcome of counter-shock.

End Tidal CO2 (ET-CO2)

Another indicator of perfusion is end tidal CO2 pressure. During normal perfusion, the partial pressure of CO2 fluctuates in the airway between the partial pressure of CO2 in the environment to the partial pressure of CO2 in the lungs. As the patient breathes in, the diaphragm contracts and creates a negative pressure in the lungs. Air from the atmosphere fills the lungs and the partial pressure in the airway decreases. End-tidal measurements of CO2 pressure is taken when the diaphragm relaxes and the lungs have completely recoiled. Because the partial pressure of CO2 at the end of the trachea is the equivalent to the CO2 partial pressure in the lungs after exhalation, and coupled with the correlation of CO2 metabolite to metabolism, ET-CO2 is a great measurement for cardio-respiratory function.

Under normal conditions, ET-CO₂ stays close to 40 mmHg in swine and humans. Gas exchange between CO₂ and O₂ in the lungs keeps the partial pressure at 40 mmHg. During exercise, cells metabolize glucose faster, thus increasing the concentration of CO₂ in the blood, thereby increasing the partial pressure of CO₂ in the lungs. A low ET-CO₂ measurement could be an indicator of poor perfusion due to limited circulation and limited transport of metabolites to the lung capillaries. During cardiac arrest, ET-CO₂ remains stagnant at 40 mmHg (an inaccurate measurement at this point), until an artificial breath is taken. The CO₂ is cleared from the lungs and ET-CO₂ levels plummet.

Taking ET-CO₂ measurements is a non-invasive procedure, only requiring a mask and a capnometer. Furthermore, previous studies have linked ET-CO₂ to CPP in a canine model (26, 27) and several clinical studies have shown ET-CO₂ influence on ROSC outcomes during CPR (28-30). A recent clinical study has shown resuscitation efforts to be unsuccessful when ET-CO₂ is less than 10 mmHg (30). Therefore ET-CO₂ might be a predictor for outcome of counter-shock and will be considered in our study. Additionally, if ET-CO₂ is deterministic of successful counter-shock, we will test for correlation with CPP in hopes to establish ET-CO₂ as a surrogate.

Amplitude Spectral Area (AMSA)

Amplitude spectral area is a frequency domain analysis of the ECG. First, a discrete Fourier transform (DFT) is performed on the ECG signal. If $x(n)$ represents the sampled ECG signal, the DFT is defined below:

$$X_k = \sum_{n=0}^{N-1} x(n) e^{-\frac{2\pi i k n}{N}}, \quad k = 0, \dots, N - 1$$

Equation 1

$$AMSA \text{ mV Hz} = \sum_{4 \text{ Hz}}^{48 \text{ Hz}} [A(i) * F(i)]$$

Equation 2

The new variable, X_k , contains spectral information of the ECG waveform. All frequency component multiples of f_s/N and their respective amplitudes are defined (f_s representing the sampling frequency) in the output. The next step sums the product of the amplitudes and frequency across frequencies from 4-48Hz which yields AMSA, as defined by equation 2.

Because AMSA is derived from the ECG waveform, the variable is non-invasive and easily acquired in the field. Studies of AMSA have shown predictive power of ROSC in both animals and humans (31-38). In a previous swine study, AMSA was significant in predicting ROSC during the first 3 minutes of resuscitation (38). Therefore AMSA will be considered in our study.

Slope

If AMSA is the frequency domain ECG waveform derivative, slope is the time domain equivalent. It represents a linearized change of amplitude of the ECG. A high value of slope is indicative of courser or healthier VF. Slope is defined as the median of

average slopes in a given interval. More specifically, the relationship is defined by equation 3.

$$Slope(\Delta t) \text{ mV/sec} = \text{Median}\{abs[x(t) - x(t - \Delta t)]/\Delta t\}$$

Equation 3

Like AMSA, during a swine study slope was a significant predictor of ROSC during the first 3 minutes of resuscitation (38). Slope is also easily derived from the ECG waveform and therefore a non-invasive variable. Slope will be included in our study.

Myocardial Infarct

This study will include a group of swine with artificial coronary infarcts. A steel plug is placed in the left anterior descending coronary 15 minutes before VF is induced. The presence of an MI can cause alterations to the VF waveform, particularly dominant and median frequencies (32,39). Additionally, infarcts limit the degree of perfusion to the ventricles during resuscitation, and represent a real life problem to consider when developing a predictive model for predicting counter-shock success.

Duration of Untreated VF

The last variable of our study is duration of VF. Effects of longer VF time on ROSC are well documented as detrimental. Ultimately, prolonged duration of VF prevents intervention further, and chances of ROSC fall 8-10% for every minute (3, 4). Additionally, emergency responders would rarely have knowledge of the arrest before arriving, potentially making the variable moot. Nevertheless it remains an essential

variable in our study to control the degree of insult resulting from cardiac arrest. There will be 2 groups delineated by VF duration: 2 minutes untreated VF versus 8 minutes untreated VF.

Purpose

Knowing when to provide the patient with a counter-shock has been difficult to define, outside of standardized algorithms such as bystander CPR protocols. However, survivability rates can be increased by timing the counter-shock to situations with a high probability of success. Our goal is to explore the dynamics of resuscitation based upon postulated variables of predictive power in order to define a model to develop optimal sequence and timing of counter-shocks. We aim to define quantitative thresholds for predictive variables leading to successful counter-shocks. Our hypothesis is that coronary perfusion pressure (CPP), end-tidal CO₂ (ET-CO₂), and the ECG waveform variables amplitude spectral area (AMSA) and slope are significant predictors for a successful counter-shock.

Overview of the Study

Original intent to search for deterministic variables for successful counter-shock came while I was executing various research protocols at the CPR research laboratory at the Sarver Heart Center. At an empirical level of observation, my colleagues and I noticed hints of correlation between CPP and successful counter-shocks. This was largely due to an early intravenous bolus of epinephrine during intervention. Animals without epinephrine administration or delayed epinephrine administration had reduced CPP levels

during CPR, and often resuscitation efforts would expire after 20 minutes. This became even more dramatic when the period of “no-treatment” was extended beyond 8 minutes. However, it became very easy to postulate the correlation of successful counter-shocks with high CPP levels as we watched the epinephrine boost CPP levels which empirically lead to successful outcomes of counter-shock.

Acquiring CPP, on the other hand, is unrealistic in emergency situations like those present during cardiac arrest. If CPP did have deterministic power, it would remain hidden during intervention unless it could be correlated to another non-invasive variable. In the midst of our empirical observations on CPP, we also observed hints of correlation between ET-CO₂ and counter-shock as well as CPP. As CPP increased during CPR, an occasional gasp from the animal would show increases of ET-CO₂ as well as a greater likelihood of successful counter-shock. Conversely, when CPP levels fell, we observed ET-CO₂ levels to parallel the effect. In the ultimate scenario of a right atrial tear during CPR, CPP and ET-CO₂ levels would plummet to minimal values and negative outcome counter-shocks were inevitable. Therefore, a relationship between CPP and ET-CO₂ was postulated and will be tested in our study.

In addition to CPP and ET-CO₂, ECG waveform variables slope and AMSA seemed equally if not more likely to be predictive of counter-shock. Previous studies by Dr. Indik et al had already shown specific relationships between AMSA and the presence of MI (39). It became the next step to test the correlation of the ECG variables to successful counter-shock.

As discussed above, the duration of untreated VF and the presence of an MI were known already to have an influence on the outcome of CPR. Therefore, we included them in our list of variables to test as biases for the outcome of counter-shock.

In conclusion, our study was formed from empirical observations during laboratory experiments as well as progression in testing ECG variables, duration of VF, and presence of MI. The first aim of our study became finding the independently predictive variables for successful counter-shock (from those selected). If ET-CO₂ and CPP were found independently significant, we would test for the level of correlation between them in order to satisfy our postulate for them being surrogates. Our second aim was to take the independently significant variables and test them in a multivariate analysis in hopes to model the undergirding dynamics for successful counter-shocks.

METHODS

This study was performed under protocol of the University of Arizona Institute of Animal Care and Use Committee and in accord with the American Physiologic Society. Swine were purchased from multiple farms in Wilcox, Arizona. They were kenneled at the Animal Care facility at the Arizona College of Medicine upon arrival.

The experiment was executed by technical personnel of the CPR research lab, under the direction of Dr. Gordon Ewy. The experiment had seven different phases:

1. Induction of Anesthesia
2. Ventilation and Maintaining Sedation
3. Instrumentation
4. Plug Placement
5. Resuscitation
6. Data Calculation
7. Statistical Analysis

Induction of Anesthesia

The first step was to anesthetize the animal and prepare it for surgery. The animal was restrained while isoflurane (5%) in 100% oxygen was delivered by nose cone. Isoflurane was used because of its minimal impairment of cardiac output (18). Once sedate, the animal was weighed and intubated by a 7.5mm endotracheal tube. The neck, a 1x1 inch portion of skin below the forearm and femur, and the upper right and lower left quadrants of the thorax were shaved. ECG pads were taped to the shaved portions of the legs in a 2-lead configuration. The surgical areas of the neck were scrubbed with alcohol and betadine. The animal was then brought to the operating room.

Ventilation and Maintaining Sedation

Sedation was maintained by a rate-volume regulated mechanical ventilator (Narkomed 2A; North American Drager, Teleford, PA). Isoflurane levels were maintained on a titrated mixture of room air and 1.5-3% anesthetic. Initial rate of ventilation was set to 12 breaths per minute at a tidal volume of 500 mL. Ventilation rate, tidal volume, and anesthetic level were adjusted to keep et-CO₂ levels at 40 +/- 3 mmHg and keep animal movement to a minimum. Prior to induced VF, anesthesia was cut to help raise aortic pressure and reduce cardiovascular impairment during resuscitation. Following resuscitation, isoflurane was brought to a concentration of 5% in 100% O₂ for 5 minutes, and then reduced to 1.5-3% in pure oxygen for the remainder of the experiment.

Instrumentation

In a sterile operating room, access to internal/external jugular veins and carotid artery were gained through a neck cut-down. The internal jugular was cannulated with a 6 french sheath, the external with a 7 french sheath, and carotid with an 8 french sheath. Ventilation lines were also coupled with a pneumotachograph and capnometer (Hans Rudolph Inc, Kansas City MI). Micromanometer-tip, solid-state pressure transducers (MCP-500; Millar Instruments, Houston, TX) were placed in the aorta and right atrium under fluoroscopy. A Swan Ganz catheter was placed in the pulmonary artery by fluoroscopy as well. With transducers, catheter, and ventilation instruments in place, electronic signals were directed to a digitizing platform (ACQ-16; Data Sciences International, St. Paul, MN). Digitized information was processed and displayed by a

computer software interface (P3P Ponemah Physiology; Data Sciences International, St. Paul, MN). ECG leads from electrodes also plugged into the digitizing platform. AED pads were placed on the animal's thorax, allowing counter-shocks to be delivered to the animal and ECG waveform acquisition by AED (Life Pak 12; Medtronic, Minneapolis, MN) at a sampling rate of 125 Hz. Data acquisition was then setup for aortic/right atrial/pulmonary artery pressures, ECG, end-tidal CO₂ (ET-CO₂), and ventilation rate.

Plug Placement

A steel plug was used to create artificial infarcts for animals randomized to acute myocardial infarction (MI). Under fluoroscopy, a guide wire (0.014") was placed in the left anterior descending coronary artery (LAD), via AR1 diagnostic catheter. The plug was then pushed down the LAD, by a pushing wire, just past the second bifurcation. The A steel plug was used to create artificial infarcts for animals randomized to acute myocardial infarction (MI). Under fluoroscopy, a guide wire (0.014") was placed in the left anterior descending coronary artery (LAD), via AR1 diagnostic catheter. The plug was then pushed down the LAD, by a pushing wire, just past the second bifurcation. The animal was allowed 15 minutes for the infarct to develop before VF was induced. Animals were randomized in a 2x2 fashion including acute infarction versus control (as well as 2 minute versus 8 minute untreated VF).

Resuscitation

Following instrumentation, , the Swan Ganz catheter was withdrawn from the external jugular and replaced by a pacing catheter electrode down the right ventricle. VF

was induced by cycling 100 Hz AC down the pacing catheter. Fibrillation was confirmed by ECG waveform inspection as well as a decline of right atrial and aortic pressures. Ventilation to the animal was stopped. The animal remained in a state of cardiac arrest for either 2 minutes or 8 minutes, depending on the group.

Resuscitation

Following instrumentation, , the Swan Ganz catheter was withdrawn from the external jugular and replaced by a pacing catheter electrode down the right ventricle. VF was induced by cycling 100 Hz AC down the pacing catheter. Fibrillation was confirmed by ECG waveform inspection as well as a decline of right atrial and aortic pressures. Ventilation to the animal was stopped. The animal remained in a state of cardiac arrest for either 2 minutes or 8 minutes, depending on the group.

At the end of the arrest phase, resuscitation efforts began immediately. A biphasic 150 Joule counter-shock was delivered at the start of intervention. A ten second observation period determined the next course of action. If the counter-shock successfully restored normal electrical activity and perfusing pressure (aortic pressure greater than 50 mmHg), resuscitation efforts stopped and return of spontaneous circulation was declared after one minute. If pulseless electrical activity (PEA) or VF was determined, active ventilation, epinephrine, and continuous compressions were started. Active mechanical ventilation was started at 10 breaths per minute at 500 mL with 100% oxygen. 1 milligram bolus of epinephrine was administered intravenously via external jugular. Manual chest compressions at a rate of 100 compressions per minute, guided by metronome, compression 1/3 the anterior-posterior diameter began as well.

After two minutes of continuous chest compressions, a ten second, hands-free, ECG observation period was observed. At the end of the duration, a determination of the ECG was made and proper course of action taken. If the animal remained in VF, a counter-shock was given, and another 10 second rhythm analysis followed. If the animal remained in VF or converted to PEA, the cycle repeated with 2 minute chest compression cycles and epinephrine delivered every 3 minutes. Resuscitation continued until 5 consecutive chest compression and shock cycles were executed.

If the animal successfully converted to a perfusing rhythm and ROSC achieved, Isoflurane was administered at 1.5-3% to sedate the animal. The animal remained under observation until pressures stabilized; after which, the animal was prepared to go off anesthesia and then placed in the kennels overnight for a 24 hour neurological assessment. Following the 24 hour assessment, animals were humanely euthanized by barbiturate overdose of 100 mg/kg.

Data Calculation

Coronary perfusion pressure, ET-CO₂, AMSA, and slope required further derivation before statistical analysis. Each variable was not graphically displayed by the software and had to be calculated.

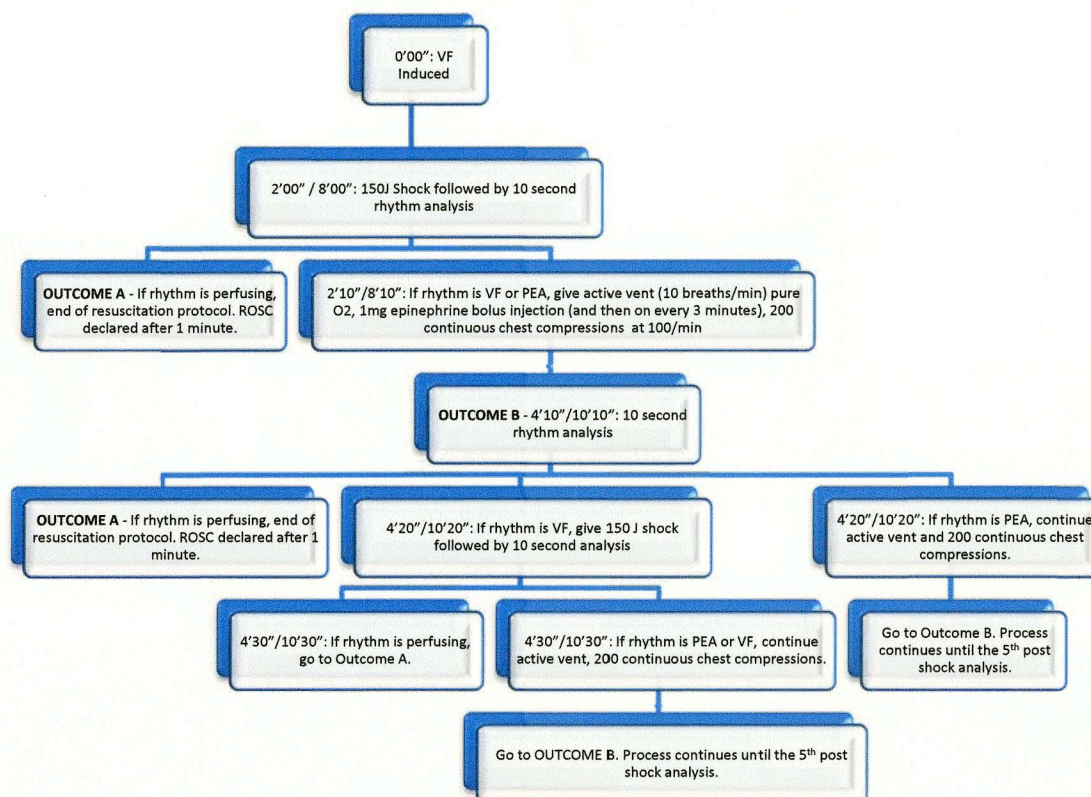


FIGURE 5: Flowchart of resuscitation protocol.

AMSA and Slope

The ECG waveform was dually recorded by P3P Ponemah Physiology and the Life Pak 12 automated external defibrillator. However, the ECG data from the AED was used to derive slope and AMSA. AMSA was calculated as the weighted sum of the product between frequency and amplitude (see equation 2 in previous section). Slope was

calculated as the median of slopes within an interval of 4.1 seconds (see equation 3 in previous section).

Information was downloaded from the AED to computer and saved in text format. The data was read by MatLab m-file for calculations explained in the introduction section (MATLAB; Mathworks, Natick, MA).

At a sampling rate of 125 Hz, the integrity of the ECG was well preserved for slope and AMSA derivation. With AMSA bandwidth of 4-48 Hz, the Nyquist frequency must be defined as greater than or equal to 48 Hz. Our system's Nyquist frequency was 62.5 Hz, thereby allowing acquisition of our bandwidth of interest.

ET-CO2

ET- CO2 was graphically shown on our software interface, however further calculation for statistical testing was necessary. The variable was derived by two separate methods: mean ET-CO2, and final ET-CO2.

Mean ET-CO2 was derived by averaging the previous 3 ET-CO2 readings before termination of chest compressions and the start of the 10 second analysis. Final ET-CO2 derivation only required taking the value immediately before the observation.

CPP

Coronary perfusion pressures were derived in three different ways, in accordance with methods previously documented (40): final end-diastole CPP, mean end-diastole CPP, and mean diastole integration. Final end-diastole CPP was obtained by taking the difference between aortic and right atrial pressures, just before the power stroke of the

left ventricle (or in our case chest compression), singly before the observation analysis and immediately after termination of chest compressions. Mean end-diastole CPP was similarly derived by averaging the previous 10 values before the analysis.



FIGURE 6: Graphical representation for final end-diastole CPP calculation.

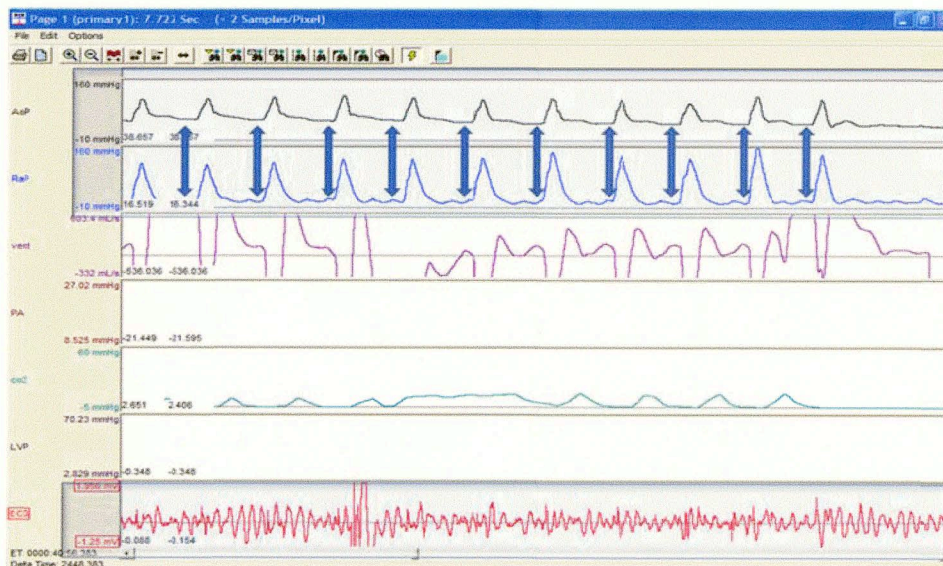


FIGURE 7: Graphical representation of mean end-diastole CPP calculation.

Deriving the mean diastole integration was more difficult. Raw sampled data from aortic and right atrial pressures were downloaded from P3P and read into a MatLab m-file. Integration boundaries were then graphically set for 10 diastole periods prior to the analysis. The upper bound was as the end-diastole point, and the lower bound was set as half the period between end diastole points. The integrations were performed numerically by Simpson's trapezoidal method and results were averaged.

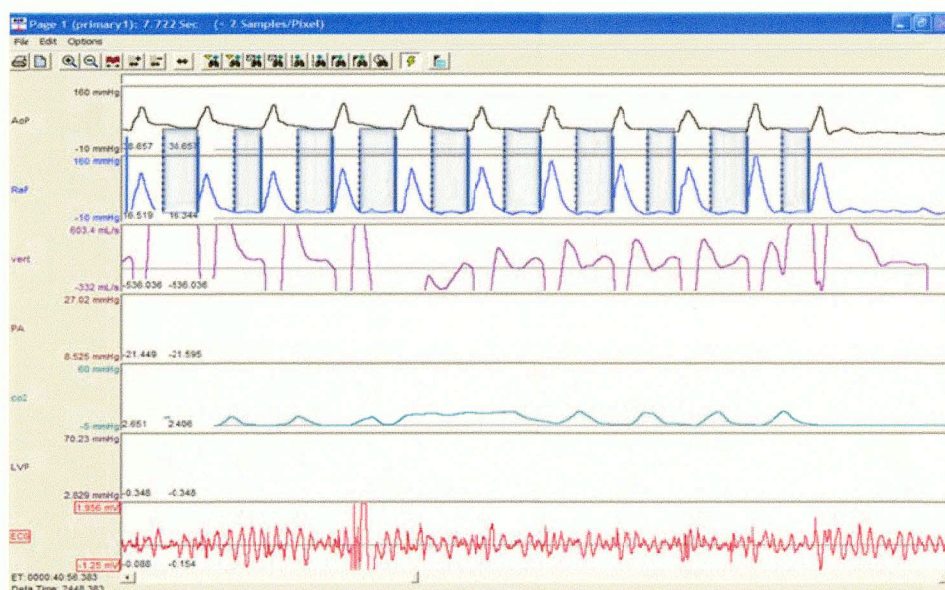


Figure 8: Graphical representation of mean end-diastole CPP integration.

There are other methods of determining the CPP in the literature. These methods have a variable means of defining the lower and upper bounds of integration by a visual inspection of the pressure tracing. These methods however are subject to error if pressure artifacts are present or other features that can confound the determination of the diastolic interval. Therefore we chose to arbitrarily set the lower bound of integration according to the period (cycle duration) of compressions. By employing this method, we are able to

avoid the miscalculation from right atrial pressure surpassing aortic pressure during the compression stroke of CPR. At that moment, CPP is negative which creates a backflow of blood. The other danger is from defining the lower boundary of integration as the start of the diastole phase. This method relies heavily on interpretation, especially when diastole begins at separate times between aortic and right atrial pressures. Our method avoids both of these concerns.

Statistical Analysis

Statistical analysis was dichotomized to represent separate populations of shocks (“2nd and higher shocks” as well as “all shocks”). CPP and ET-CO₂ variables are not applicable to the “all shocks” population because there is no reading available during the first shock. A tertile model was set up for each set of shocks and regressions were performed. All variables were analyzed in the “2nd and higher shocks” set. Only AMSA, slope, MI, and duration of VF were analyzed in the “all shocks” set.

Univariate logistic regression was performed in Stata on all variables of interest (Stata LP; Stata 10.0, College Station, TX). Variables were put into tertiles and tested as univariate predictors for successful counter-shock. Variables found significant ($p < 0.1$) were tested in the multivariate logistic regression. Variables that remained predictive of successful outcome of counter-shock were analyzed by ROC with sensitivity and specificity. In every test, random effects were assumed due to the repeated measures of multiple shocks per animal subject. Stata utilized the Guass-Mermitte quadrature approximation in the random effects model in our analysis.

RESULTS

The population of my study was approximately uniform by weight and age. For 31 animals, we counter-shocked 66 times. Of the 66, 31 were first shocks leaving the other 35 for analysis (CPP and CO2 measurements were not applicable to first shocks).

The populations of the groups were not uniform. Initially, we planned on having equally distributed groups. As the study began, we observed that the 2 minute arrest group was easily resuscitated. They required no more than 2 shocks. Therefore, the 2 minute group was discontinued, but will not be ignored in our analysis. Table 1 shows the baseline characteristics of each group. The remainder of this section will present results from the “2nd shock and higher” set, followed by the “all shocks” population set. Univariate and multivariate regression will be performed for each section, followed by ROC results for independent variables.

2nd and Higher Shocks - Univariate Analysis

Variables were divided into tertiles and then logistically analyzed for variance for predicting a successful counter-shock (tertiles are defined in table 2). Successful counter-shock was defined as a shock that converted VF to a perfusing rhythm or to PEA and progressed to a perfusing rhythm within 2 minutes.

Group	Size	Weight	Aortic Systole	Aortic Diastole	Right Atrial Systole	Right Atrial Diastole	Cardiac Output	Wedge
8min Normal	10	25.02 +/- 2.46 Kg	86.64 +/- 9.71 mmHg	61.61 +/- 9.39 mmHg	9.81 +/- 3.84 mmHg	6.07 +/- 4.07 mmHg	2.93 +/- 0.51 mmHg	7.95 +/- 3.19 mmHg
8min MI	11	25.43 +/- 2.26 Kg	83.96 +/- 11.91 mmHg	58.33 +/- 11.22 mmHg	17.61 +/- 18.81 mmHg	10.07 +/- 6.53 mmHg	2.86 +/- 0.50 mmHg	7.73 +/- 3.03 mmHg
2min Normal	7	25.56 +/- 2.84 Kg	95 +/- 10.69 mmHg	66.71 +/- 7.74 mmHg	9.29 +/- 1.98 mmHg	5.14 +/- 2.12 mmHg	3.12 +/- 0.30 mmHg	6.24 +/- 2.08 mmHg
2min MI	3	22.83 +/- 1.15 Kg	92.66 +/- 14.01 mmHg	69.33 +/- 14.57 mmHg	14.66 +/- 9.81 mmHg	11.33 +/- 8.39 mmHg	2.48 +/- 0.26 mmHg	7.68 +/- 2.81 mmHg

TABLE 1: Baseline Populations and Hemodynamics

CPP Variables

Single variable logistic regression on Final CPP yielded non-significant results (P=0.202 OR=75.335 CI: [0.098 57684.25] middle tertile; P=0.826 OR=1.617 CI: [0.022 116.805] upper tertile). Lack of strength in the odd ratio and p-value gave reason to dismiss the variable for further testing in a multivariate test.

Mean CPP did not test as a significant predictor of successful counter-shock as well (P=0.079 OR=87.166 CI: [0.597 12719.37] middle tertile, P=0.471 OR=3.556 CI: [0.113 111.879] upper tertile). The Final CPP and Mean CPP variables both provided significance in one tertile, but lacked in the other tertile.

Variable	Definition	1 st Tertile	2 nd Tertile	3 rd Tertile
Final CPP (mmHg)	A single CPP measurement taken just after the final chest-compression and at the start of analysis.	$5.552 \leq x < 25.079$	$25.079 \leq x < 37.727$	$37.727 \leq x \leq 89.354$
Mean CPP (mmHg)	The average of 10 CPP measurements taken just prior to the rhythm analysis (Includes the Final CPP reading).	$3.4471 \leq x < 27.8353$	$27.835 \leq x < 37.193$	$37.193 \leq x \leq 80.839$
MDI CPP (mmHg)	Mean diastole integration CPP integrates the diastolic difference between aortic and right atrial pressure waves for the 10 compressions prior to the rhythm analysis.	$2.3043 \leq x < 8.4675$	$8.468 \leq x < 12.395$	$12.395 \leq x \leq 22.759$
Final CO2 (mmHg)	The end-tidal CO2 measurement taken before rhythm analysis.	$7.05 \leq x < 12.32$	$12.320 \leq x < 15.00$	$15.00 \leq x \leq 32.70$
Mean CO2 (mmHg)	The average of the 3 end-tidal CO2 measurements taken before rhythm analysis.	$8.94 \leq x < 13.03$	$13.030 \leq x < 15.90$	$15.90 \leq x \leq 32.73$
Slope (Volts/second)	The median slope of the ECG waveform over 4 seconds.	$1.088 \leq x < 2.737$	$2.737 \leq x < 3.635$	$3.635 \leq x \leq 6.119$
AMSA (milliVolt-Hz)	The spectral area of power between 4-48 Hz.	$11.509 \leq x < 29.012$	$29.012 \leq x < 37.406$	$37.406 \leq x \leq 58.333$

TABLE 2: Tertile Divisions of variables and their description (Duration of VF and MI variables were not applicable for tertiles).

Integration of CPP was not significant ($P=0.202$ OR=75.334 CI: [0.098 57684.25] middle tertile; $P=0.826$ OR=1.617 CI: [0.022 116.805] upper tertile). We observed similar results with the other CPP variables, and none satisfied the margin of significance required for multivariate analysis. Therefore, mean diastole integration CPP was dismissed for multivariate testing, along with the other CPP variables.

Furthermore, we observed strong linearity between CPP variables, as expected. Figures 9 and 10 show linearity between CPP variables. Spearman rank coefficients and covariance was calculated between CPP variables and the results are shown in table 3. Table 4 displays a summary of logistic regression results.

Variables	Final CPP	Mean CPP	MDI CPP
Final CPP	1		
Mean CPP	0.9659	1	
MDI CPP	0.9486	0.9899	1

TABLE 3: Spearman rank coefficients for CPP variables.

Variable	Odd Ratio	P	95% Confidence Interval
Final CPP (Middle)	75.33474	0.202	0.098386, 57684.25
Final CPP (Upper)	1.617174	0.826	0.02239, 116.8046
Mean CPP (Middle)	87.16582	0.079	0.5973471, 12719.37
Mean CPP (Upper)	3.556466	0.471	0.1130543, 111.8795
MDI CPP (Middle)	75.33474	0.202	0.098386, 57684.25
MDI CPP (Upper)	1.617174	0.826	0.02239, 116.8046

TABLE 4: Summary of CPP variables as predictors for successful counter-shock.

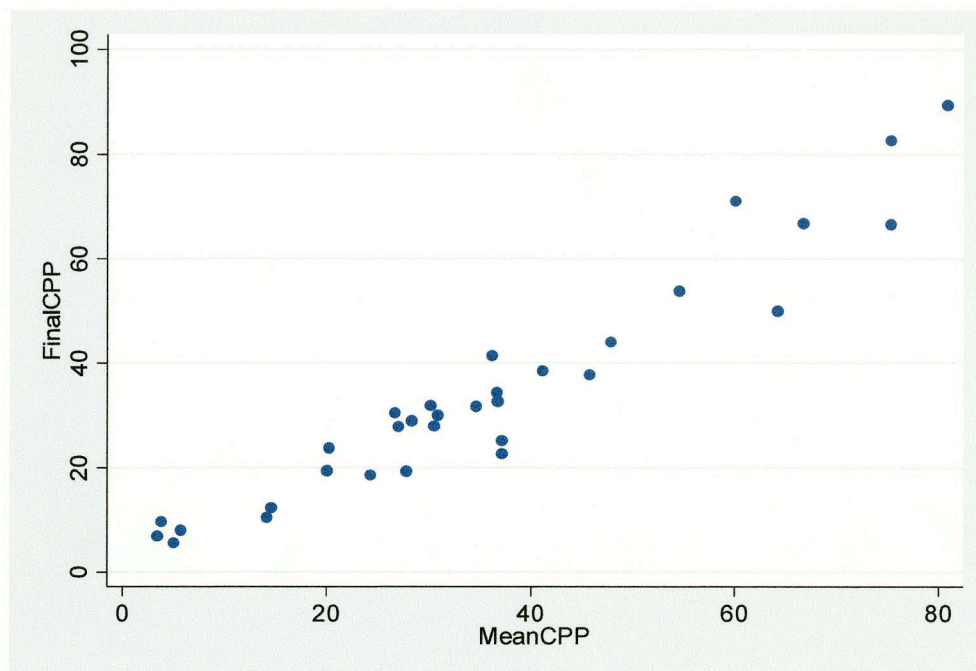


FIGURE 9: Final CPP versus Mean CPP

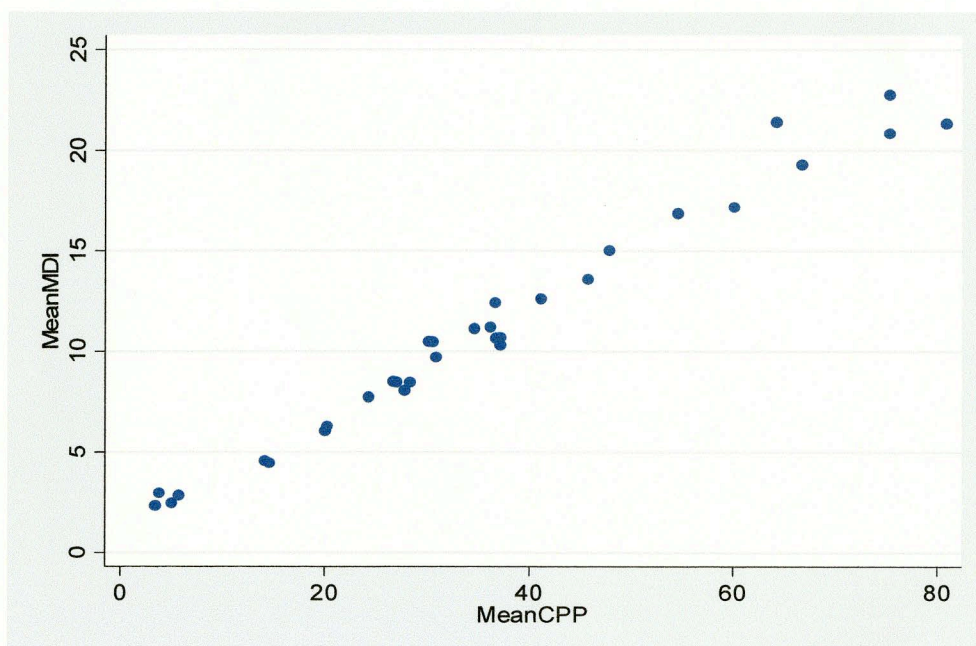


FIGURE 10: MDI CPP versus Mean CPP

In conclusion, there is no significance measured for CPP variables as a predictor.

Box-whisker plots in figures 11 through 13 suggest CPP variables are not predictive of positive outcome counter-shock.

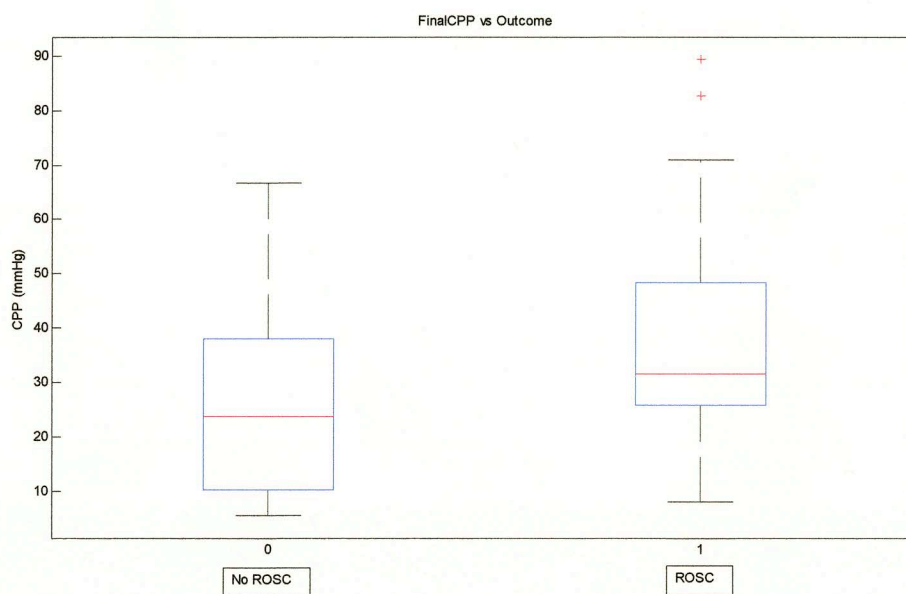


FIGURE 11: Box-Whisker Plot of Final CPP

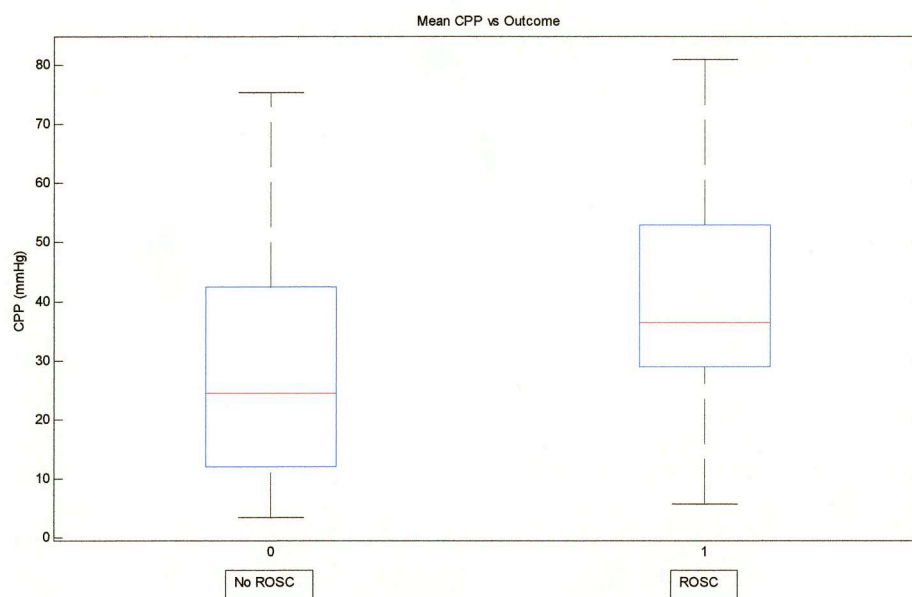


FIGURE 12: Box-Whisker Plot of Mean CPP

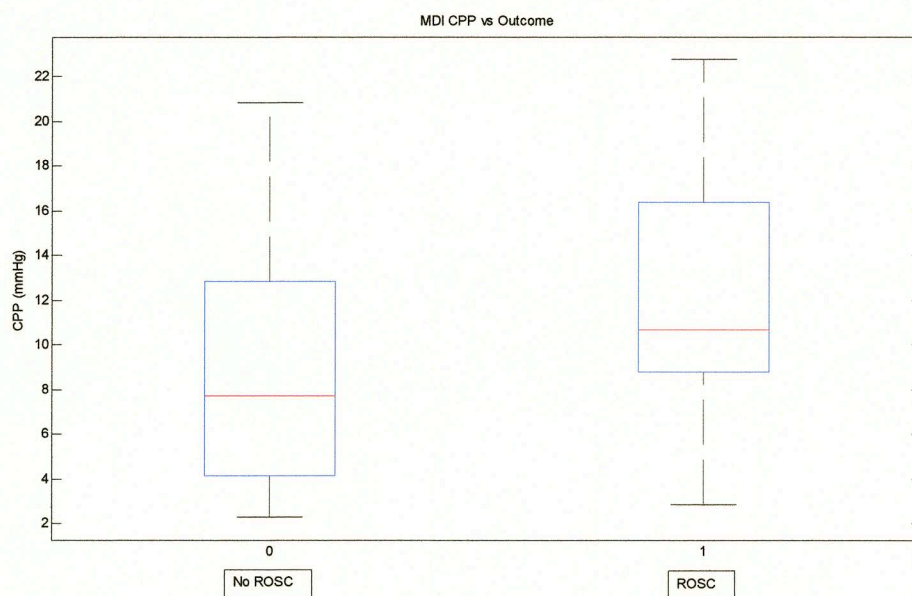


FIGURE 13: Box-Whisker Plot of MDI CPP

CO2 Variables

Final CO2 was not significant (P=0.699 OR=0.590 CI: [0.041 8.535] middle tertile; P=0.265 OR=0.106 CI: [0.002 5.488] upper tertile). However, increased values of Final CO2 yielded a better p-value. Mean CO2 was not significant either (P=0.975 OR=1.051 CI: [0.045 24.414] middle tertile; P=0.279 OR=0.279 CI: [0.004 19.400] upper tertile). Given a tertile model, there was not enough conformity in variance to suggest either CO2 variable as a predictor of a successful counter-shock.

Like the CPP variables, the CO2 variables are also highly correlated. Table 5 lists their Spearman rank coefficients and covariance's. Table 6 gives a summary of results for the logistic regression.

Variable	Final CO2	Mean CO2
Final CO2	1	
Mean CO2	0.9463	1

TABLE 5: Spearman rank coefficients for CO2 variables.

Variable	Odd Ratio	P	95% Confidence Interval
Final CO2 (Middle)	0.590	0.699	0.041, 8.535
Final CO2 (Upper)	0.106	0.265	0.002, 5.488
Mean CO2 (Middle)	1.051	0.975	0.045, 24.414
Mean CO2 (Upper)	0.279	0.555	0.004, 19.400

TABLE 4: Summary of CO2 variables as predictors for successful counter-shock.

In conclusion, neither CO₂ variable will be included in the multivariate logistic regression. Figures 14 and 15 are box-whisker plots of CO₂ variables versus outcome of shock and they confirm, by visual inspection, a lack of predictive ability.

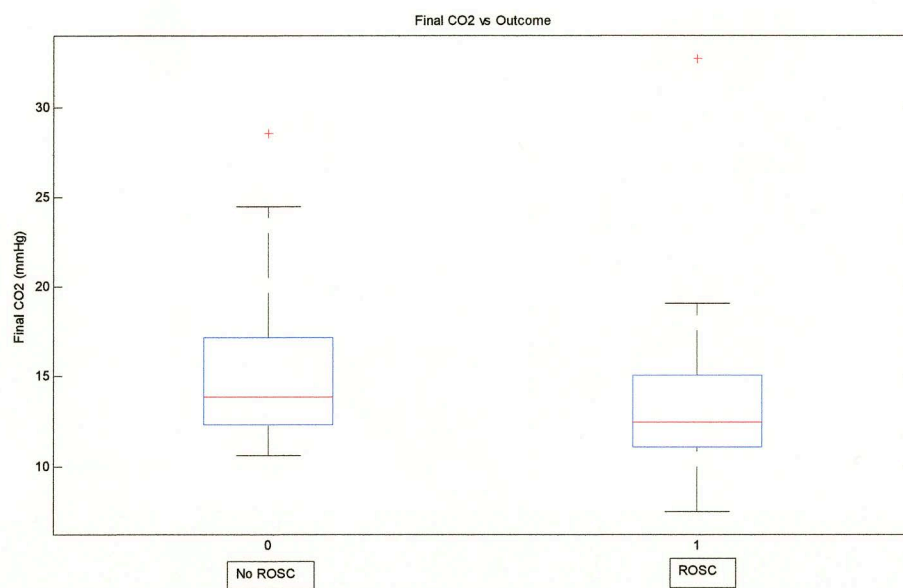


FIGURE 14: Box-whisker plot of Final CO₂.

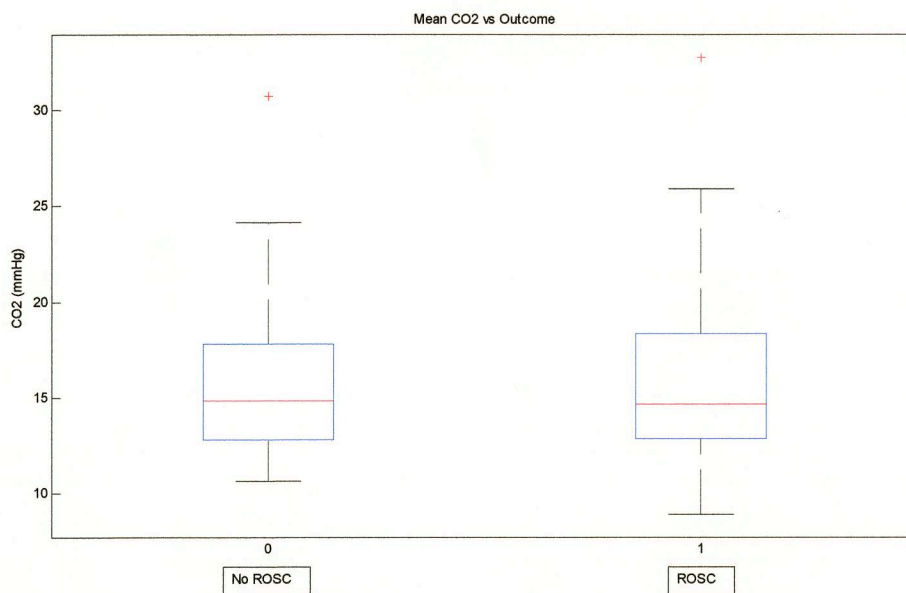


FIGURE 15: Box-whisker plot of Mean CO2.

ECG Waveform Variables

Slope was tested significant during univariate analysis ($P=0.071$ OR=6.999 CI: [0.849 57.680] lower tertile; $P=0.006$ OR=47.585 CI: [3.063 739.249]). Both tertiles were easily within our margin of $P=0.1$, and slope will be included in the multivariate logistic regression.

Results for AMSA as a predictor for successful counter-shock were significant ($P=0.290$ OR=2.667 CI: [0.434 16.39] middle tertile; $P=0.009$ OR=26.667 CI: [2.309 307.954] upper tertile). The middle tertile did not fall within our margin; however, there is a strong correlation between AMSA and slope variables. A Spearman rank coefficient was calculated as 0.8651, arguably surrogate variables. Table 7 summarizes the coefficient

and covariance. Figure 16 also shows the linearity between variables. Therefore, both variables will be tested independently in the multivariate regression analysis. Table 8 displays a summary of the univariate analysis and figures 17 and 18 give box-whisker representations of AMSA and slope per outcome of shock.

Variable	Slope	AMSA
Slope	1	
AMSA	0.8651	1

TABLE 7: Spearman rank coefficient for ECG variables.

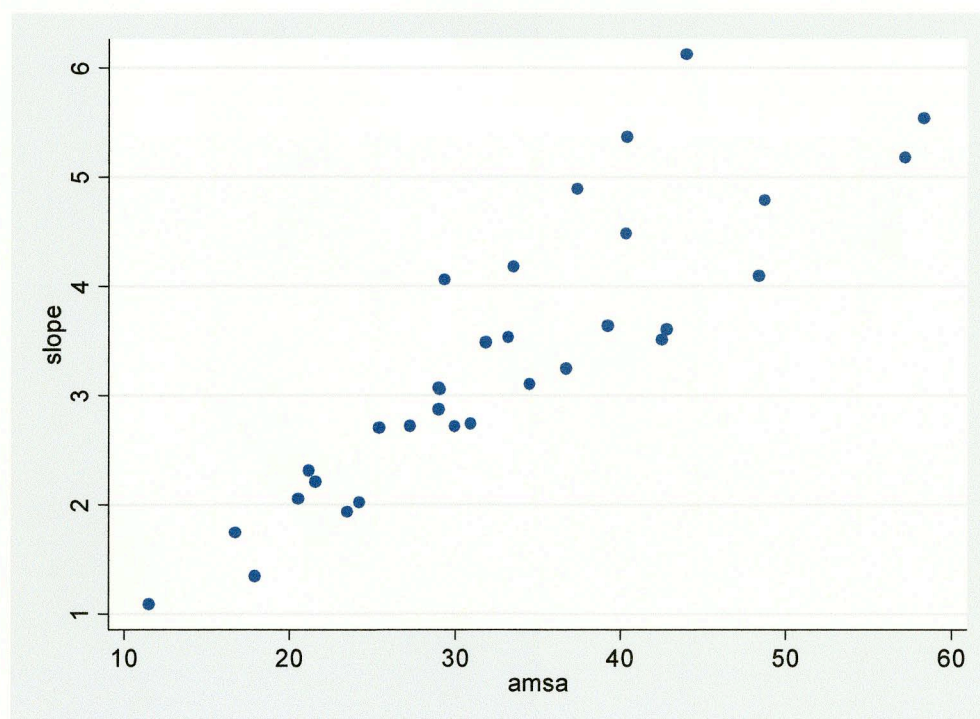


FIGURE 16: Slope vs AMSA

Variable	Odd Ratio	P	95% Confidence Interval
Slope (Middle)	6.999	0.071	0.849, 57.680
Slope (Upper)	47.585	0.006	3.063, 739.249
AMSA (Middle)	2.667	0.290	0.434, 16.39
AMSA (Upper)	26.667	0.009	2.309, 307.954

TABLE 8: Summary of waveform variables as predictors for successful counter-shock.

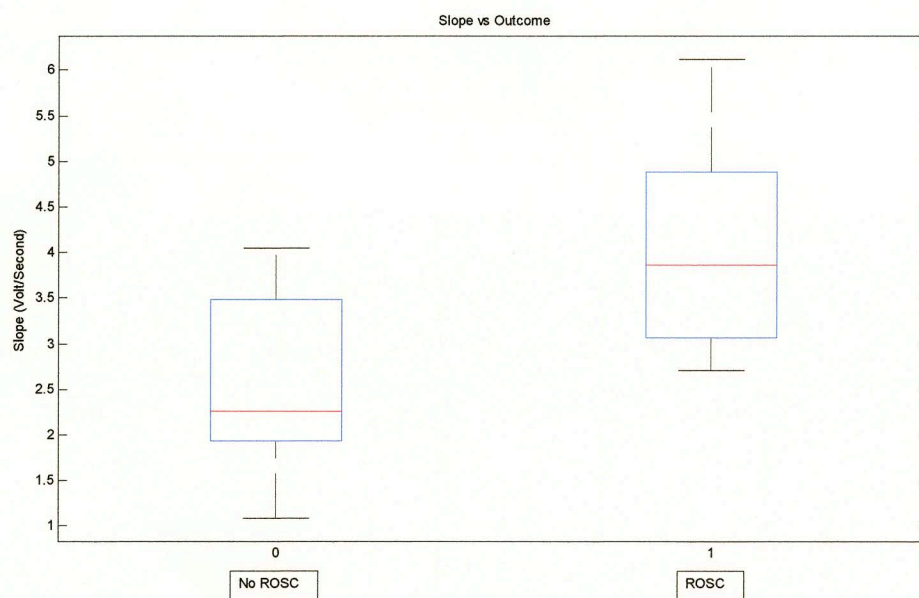


FIGURE 17: Box-whisker plot of Slope

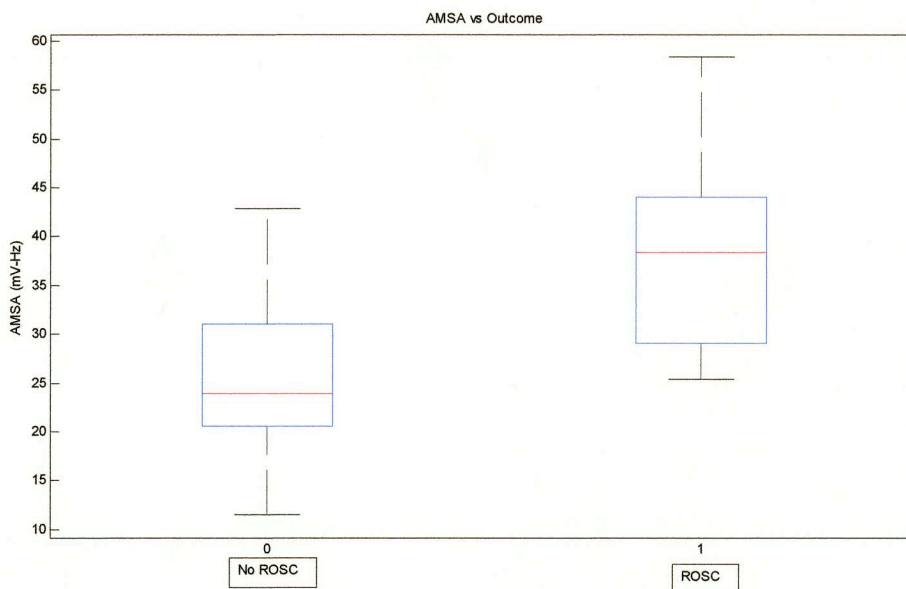


FIGURE 18: Box-whisker plot of AMSA

In conclusion, both ECG waveform variables were very predictive of successful counter-shock and both will be included for multivariate regression.

Binary Variables

Duration of VF and MI, both variables being incompatible to a tertile model, were tested by logistic regression via categorical model. When excluding all of the first shocks, the MI analysis did not converge. The cause is due to a high percentage of animals without an MI returning to a perfusing rhythm on the second shock (11/11 without MI returned on the second shock).

Duration of VF was also analyzed without first shocks ($P=0.999$ OR= $<<0$ CI: [0 inf]). The test nearly did not converge (4/4 animals in the 2 minute group returned on the second shock). Table 9 summarizes the results for the binary variables.

Variable	Odd Ratio	P	95% Confidence Interval
MI vs Control <i>2nd and higher shocks</i>			
8 minute vs 2 minute <i>2nd and higher shocks</i>	$<< 0$	0.999	0, inf

TABLE 9: Summary of binary variables as predictors for successful counter-shock.

In conclusion, MI and the duration of VF were not significant in the “2nd and higher” shock population and could not be included in the associated multivariate regression.

2nd and Higher Shocks - Multivariate Analysis

The only variables found significant predictors during the “2nd and higher” shock set were AMSA and slope. Due to the high correlation between the two variables, multivariate analysis was not valid.

All Shocks – Univariate Analysis

Like the “2nd and higher” shocks population, variables of AMSA, slope, MI, and duration of VF were tested for significance to predict successful counter-shocks. AMSA and slope tertile delineations were reassessed and results are displayed in table 10.

Variable	1 st Tertile	2 nd Tertile	3 rd Tertile
Slope (Volts/second)	$0.419 \leq x < 1.988$	$1.988 \leq x < 3.098$	$3.098 \leq x \leq 6.119$
AMSA (milliVolt-Hz)	$4.485 \leq x < 20.382$	$20.382 \leq x < 29.989$	$29.989 \leq x \leq 58.333$

TABLE 10: Tertile values for AMSA and slope in the “all shocks” population.

ECG Waveform Variables

AMSA and slope were each tested for significance to predict successful counter-shocks in the extended population. Slope was significant (P=0.038 OR=10.945 CI: [1.139 105.146] middle tertile; P=0.003 OR=67.897 CI: [4.205 1096.26] upper tertile) as well as AMSA (P=0.065 OR=7.569 CI: [0.880 65.122] middle tertile; P= 0.007 OR=35.434 CI: [2.709 463.539] upper tertile). Table 11 summarizes the results.

Variable	Odd Ratio	P	95% Confidence Interval
Slope (Middle)	10.945	0.038	1.139, 105.146
Slope (Upper)	67.897	0.003	4.205, 1096.26
AMSA (Middle)	7.569	0.065	0.880, 65.122
AMSA (Upper)	35.434	0.007	2.709, 463.539

TABLE 11: Results of the univariate logistic regression for AMSA and slope for the extended population of shocks.

Binary Variables

MI and duration of VF variables were reassessed in the “all shocks” population and both variables were significant for predicting successful counter-shock. Both

variables were included in the multivariate logistic regression. Results are summarized in table 12.

Variable	Odd Ratio	P	95% Confidence Interval
MI vs Control <i>All Shocks</i>	0.299	0.020	0.108, 0.829
8 minute vs 2 minute <i>All shocks</i>	0.198	0.013	0.055, 0.714

TABLE 12: Results of the univariate logistic regression for MI and duration of VF for the extended population of shocks.

All Shocks – Multivariate Analysis

AMSA, slope, MI, and the duration of VF were considered potential parameters for the multivariate analysis. Because AMSA and slope have a correlation to each other, each ECG variable was tested without the other. Results are shown in table 13.

Our first observation was AMSA and slope remained significant predictors of successful counter shock in the multivariate setting. Secondly, the presence of an MI though significant in univariate analysis, was no longer significant in the multivariate. Lastly, the duration of VF remained a significant predictor of successful counter-shock.

Variable	Odd Ratio	P	95% Confidence Interval
Test 1: Slope			
Slope (Middle)	7.205	0.029	1.224, 42.415
Slope (Upper)	33.894	0.000	5.142, 223.424
MI (Animal had infarct)	0.529	0.374	0.130, 2.151
Time in VF (8min)	0.194	0.067	0.033, 1.120
Test 2: AMSA			
AMSA (Middle)	3.975	0.091	0.802, 19.692
AMSA (Upper)	16.921	0.001	3.249, 88.140
MI (Animal had infarct)	0.480	0.267	0.132, 1.753
Time in VF (8min)	0.179	0.043	0.034, 0.949

TABLE 13: Summary of multivariate logistic regression of AMSA, slope, MI, and duration of VF.

Sensitivity and Specificity Analysis

Slope, AMSA, and time in VF were shown to be significant predictors of successful counter-shock in the multivariate analysis. We then sought further delineation of predicting successful counter-shocks with our significant quantitative variables. Both variables were tested (in quantitative format) for specificity and sensitivity as predictors of successful counter-shock. Time in VF was not included in the specificity/sensitivity analysis because the variable is categorical. Additionally, the outcome of this analysis could only provide an approximation for the true associated curves of specificity and sensitivity due to the repeated measures of making up the population of multiple shocks per animal. Results are displayed in figures 19 through 22. Figures 19 and 20 portray the analysis done with the initial population “2nd shocks and higher.” Figures 21 and 22

portray the results yielded from the extended population including all shocks. Table 14 shows the area under the curves.

Variable	Area Under Curve	95% Confidence Interval
Slope <i>2nd Shock and Higher</i>	0.8611	0.732, 0.991
AMSA <i>2nd Shock and Higher</i>	0.8492	0.710, 0.988
Slope <i>All Shocks</i>	0.8561	0.762, 0.950
AMSA <i>All Shocks</i>	0.830	0.726, 0.934

TABLE 14: Areas under the curves for sensitivity/specificity analysis of AMSA and slope.

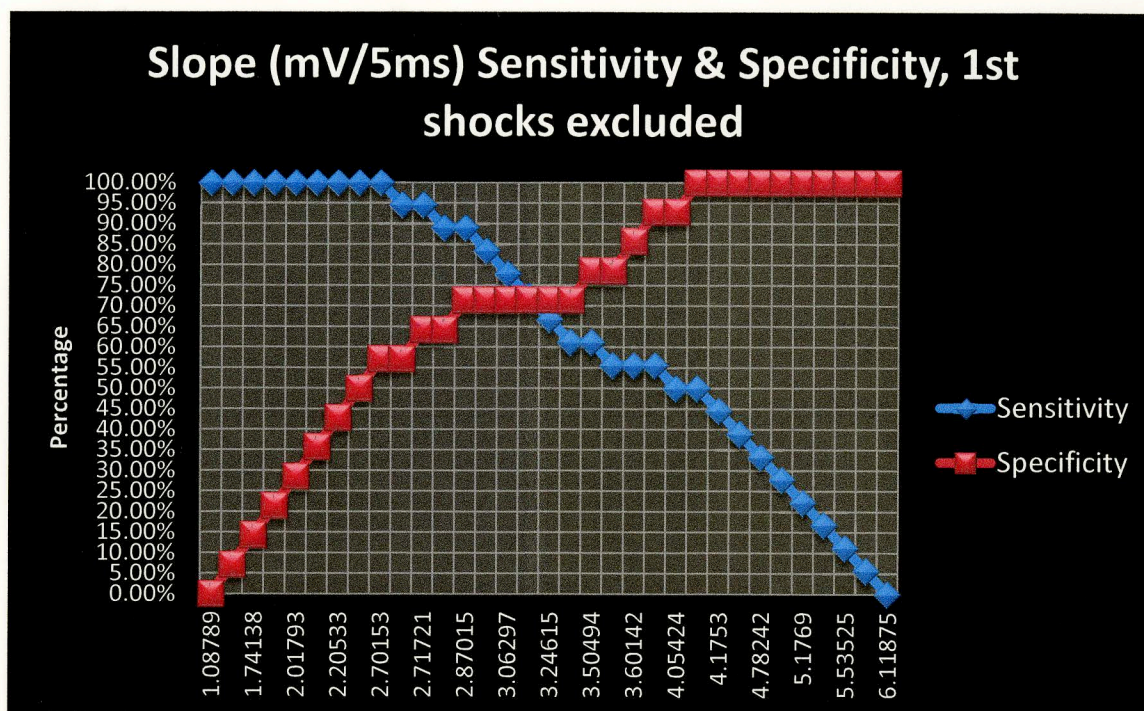


FIGURE 19: Sensitivity and specificity as a function of slope, created from 1st shock excluded data.

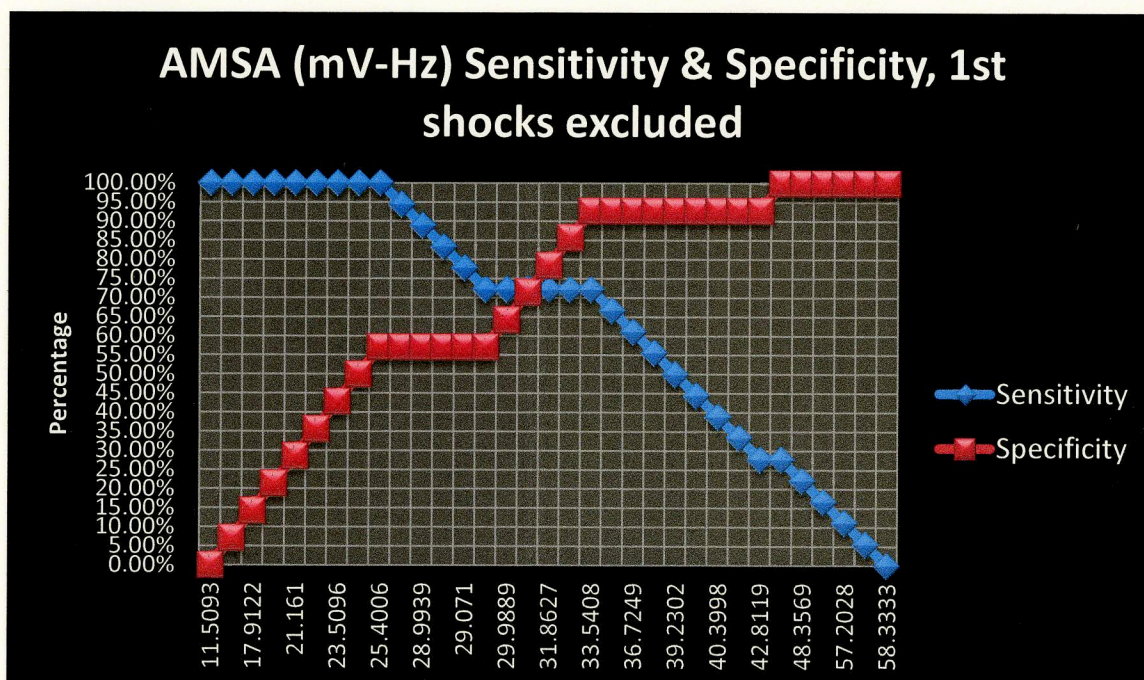


FIGURE 20: Sensitivity and specificity as a function of AMSA, created from 1st shock excluded data.

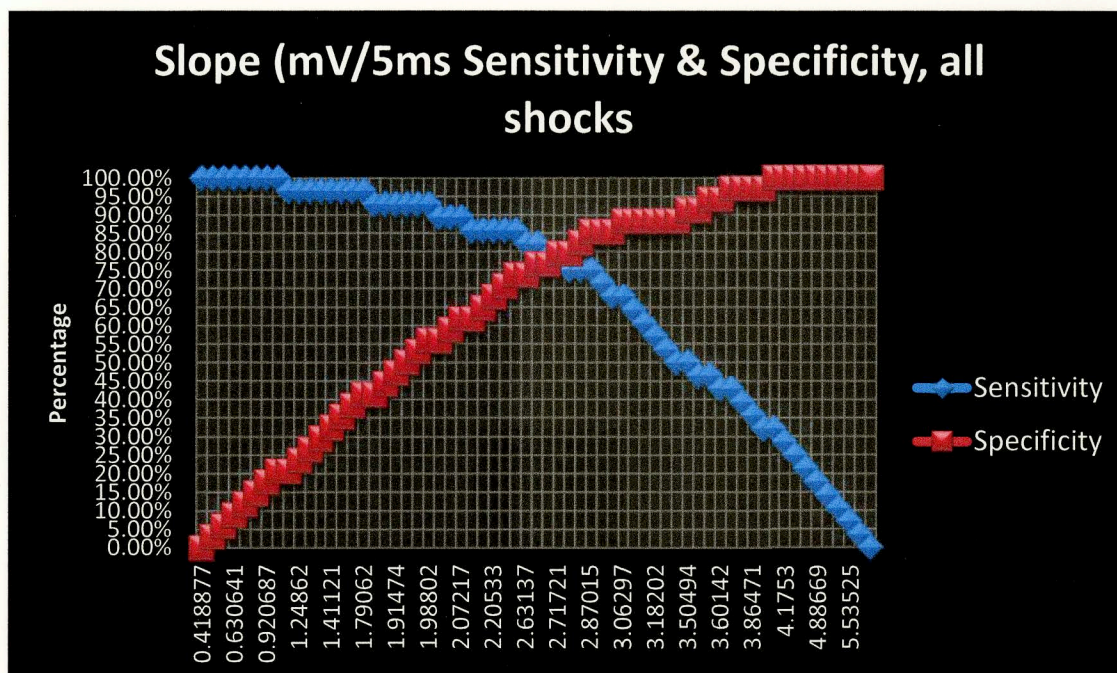


FIGURE 21: Sensitivity and specificity as a function of Slope, created from data including all shocks.

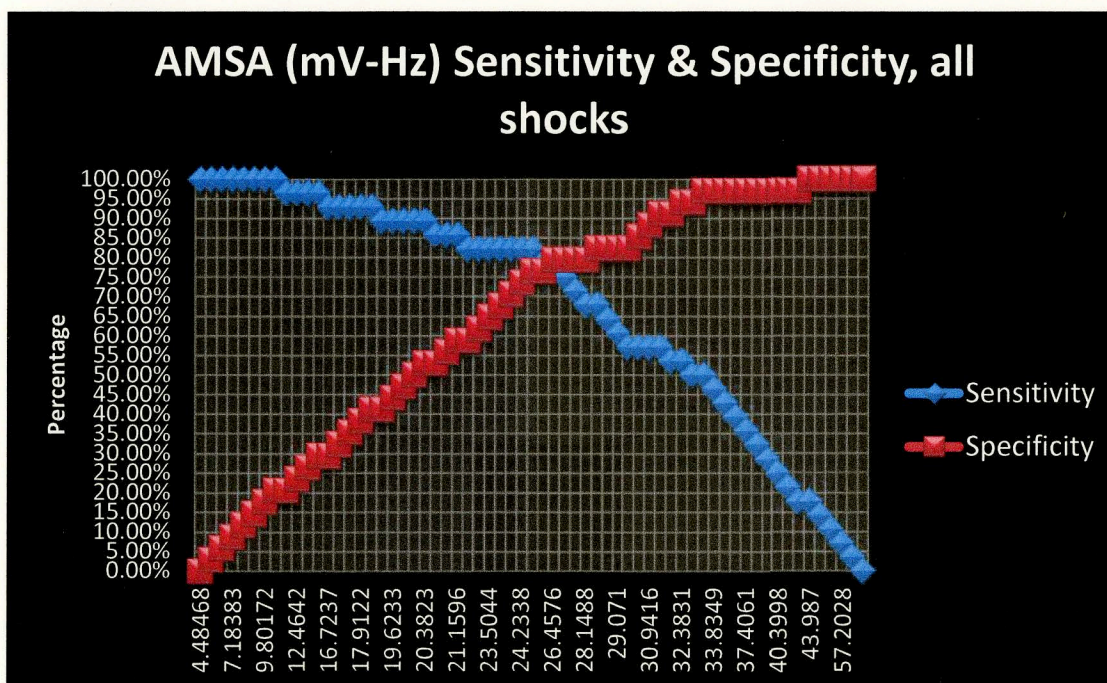


FIGURE 22: Sensitivity and specificity as a function of AMSA, created from data including all shocks.

DISCUSSION

For a swine model of VF cardiac arrest, we have successfully isolated independently significant predictors of successful counter-shock, defined as a counter-shock which returns the pig to an unassisted perfusing rhythm within 2 minutes of the shock. We have also tested the predictive ability of the significant variables when combined into a multivariate model through logistic regression. Lastly we analyzed key predictive variables in a ROC analysis, thereby outlining sensitivity and specificity given thresholds.

Our findings show slope and AMSA to be significant predictors, both independently and in a multivariate model including MI and the duration of VF. Previous studies involving ECG waveform analysis during VF including AMSA and slope have found the variables predictive of ROSC in humans (31-34) and animals (35-37). Our investigation agrees with these studies; however our model differs slightly per resuscitation protocol as well as our study focusing on shock outcomes during prolonged resuscitation efforts.

Our hypothesis was that we expected CPP to be a significant predictor of ROSC following counter-shock, complimenting previous investigations in humans (22) and animals (23-25). Our study did not yield comparable results. Although CPP levels were elevated non-significantly prior to chest compression and shock cycles, the logistic regression never yielded significance. In the human study (22), 79% of cardiac arrest victims achieved ROSC with a CPP greater than 25 mmHg. Similarly 17 out of 23 shocks with CPP levels greater than 25 mmHg in our study resulted in ROSC. But after our

analysis, we observed CPP to have less bearing on outcome if the cardiac arrest duration was short (2 minute group). Furthermore, our investigation had significant differences compared to previous studies in that our focus was on the immediate outcome shock-by-shock during resuscitation compared to analysis based on the resuscitation outcome as a whole. Additionally our investigation utilized administration of epinephrine by bolus every 3 minutes throughout resuscitation as well as creating myocardial infarcts in part of the population. Lastly, our study involved high performance chest compressions given by trained and experienced technicians accustomed to the swine model.

We found neither set of variables (CPP and ET-CO₂) independently significant for predicting counter-shock. Previous investigations have shown threshold et-CO₂ levels to be correlated with ROSC (28-30) in observational studies as well as correlated to CPP involving canine models (26, 27). An observational analysis of cardiac arrest victims, with or without VF, showed positive ROSC of all subjects for et-CO₂ levels above 10 mmHg. Again, the nature of our protocol and focus differed from these other investigations. Our focus was toward the immediate outcome of the shock. Our study's investigation also utilized high performance chest compressions and administration of epinephrine.

The presence of an acute MI had predictive power when all shocks were considered; however, when the variable was included in the multivariate regression, the variable became no longer significant. In our study, every animal without an acute MI returned to ROSC by the second shock. Furthermore acute myocardial infarction

resuscitation times was longer than non-MI times, requiring more shocks to achieve ROSC. But in the end, MI dropped out of significance when included in a multivariate logistic regression, which serves as an advantage due to the difficulty to ascertain the presence of an MI induced VF cardiac arrest in the field.

Lastly, the duration was shown to be a significant predictor of successful counter-shock in the univariate as well as multivariate analysis. The variable was added to find if the VF waveform or any other parameter could give further predictive value. There have been many investigations suggesting the decreasing likelihood of the animal ultimately achieving ROSC based on the duration of VF (3, 4). Our findings were comparable with overwhelmingly successful ROSC in swine with only 2 minute insults. Therefore, the duration of VF is a meaningful predictable, as long as the arrest is witnessed and information of the victims duration of arrest is available to emergency responders.

Limitations

A key limitation of our study is the anatomical differences between human and swine models. Additionally, methods of chest compression are subtly different where technicians must adapt their technique to conform to the swine's raised chest. Furthermore, outcomes in human arrest include 24 hour survival as well as hospital discharge and evaluation. The swine in our study received a 24 hour neurological assessment, which nearly all were able to achieve due to high performance CPR. Human treatment also includes a greater degree of variability of standards as well as patient diversity, thereby creating the potential for uncontrolled variables. CPP was also

collected offline preventing any real-time analysis from being performed; this is not a limitation but an acknowledgment that results were analyzed retrospectively as opposed to prospectively. As mentioned in the results section, all swine which did not receive an acute MI or fell into the 2 minute duration of VF groups were overwhelmingly resuscitated early, preventing a multivariate regression including MI and VF time without first shocks from converging. Lastly, the use of epinephrine during the resuscitation may have affected the outcome of ET-CO₂ because of its known effects of shunting blood away from the lungs.

Future Work

After isolating slope and AMSA as key predictors of successful counter-shock, the next step will be testing their predictive power based upon varying levels of sensitivity and specificity. We have already begun instrumentation on a project that will collect AMSA and slope ECG derivatives real-time during resuscitation. The system includes a Zoll defibrillator that provides shock and analyzes ECG rhythm from the ECG pads at 250 Hz. The values of the variables will then be used to decide whether to intervene with shock.

Conclusion

Our analysis concludes AMSA and slope to be predictors of a counter-shock resulting in a perfusing rhythm within 2 minutes of the shock from prolonged untreated VF. Additionally MI and the duration of VF are also predictors when considering all shocks give to the animals, but MI fell out of significance during the multivariate logistic

regression. Lastly, CPP and et-CO₂ are not predictors of successful outcome based on counter-shocks.

REFERENCES

1. Heart Disease and Stroke Statistics_2010 Update: A Report From the American Heart Association. *Circulation*. 2010;121:e46-e215; originally published online Dec 17, 2009;
2. Coronary Heart Disease and Prevention in the United States; Jeremiah R. Brown, PhD, Gerald T. O'Connor, PhD. *N Engl J Med*. 2010; 362:2150-2153 June 10, 2010.
3. Estimating Effectiveness of Cardiac Arrest Interventions. Valenzuela T, Roe D, Cretin S, Spaite D, Larsen M. *Circulation*. 1997;96:3308-3313
4. Predicting survival from Out-of-Hospital Cardiac Arrest. Larsen MP, Eisenburg MS, Cummins RO, Hallstrom AP. *Ann Emerg Med*. 1993;22:1652-1658.
5. Ventricular Fibrillation of Long Duration Abolished by Electric Shock. C. S. Beck, M.D.; W. H. Pritchard, M.D.; H. S. Feil, M.D. *J Am Med Assoc*. 1947;135(15):985-986.
6. Multicenter, Randomized, Controlled Trial of 150-J Biphasic Shocks Compared With 200- to 360-J Monophasic Shocks in the Resuscitation of Out-of-Hospital Cardiac Arrest Victims. Thomas Schneider, MD; Patrick R. Martens, MD; Hans Paschen, MD; Markku Kuisma, MD; Benno Wolcke, MD; Bradford E. Gliner, MS; James K. Russell, PhD; W. Douglas Weaver, MD; Leo Bossaert, MD; Douglas Chamberlain, MD; for the Optimized Response to Cardiac Arrest (ORCA) Investigators. *Circulation*. 2000;102:1780-1787

7. Accepted, controversial, and speculative aspects of ventricular defibrillation.
Crampton R. *Prog Cardiovasc Dis*. 1980;23:167–186.
8. Ventricular defibrillation—a comparative trial using. Weaver WD, Cobb LA, Copass MK, et al. 175-J and 320-J shocks. *N Engl J Med*. 1982;307:1101–1106.
9. Effect of ventricular shock strength on cardiac hemodynamics. Tokano T, Bach D, Chang J, et al. *J Cardiovasc Electrophysiol*. 1998;9:791–797.
10. Defibrillation with low-energy biphasic waveform reduces the severity of post-resuscitation myocardial dysfunction after prolonged cardiac arrest. Tang W, Weil MH, Sun S, et al. *J Am Coll Cardiol*. 1999;34:815–822.
11. High-energy defibrillation increases the severity of postresuscitation myocardial dysfunction. Xie J, Weil MH, Sun S, et al. *Circulation*. 1997;96:683–688.
12. Relation between shock-related myocardial injury and defibrillation efficacy of monophasic and biphasic shocks in a canine model. Osswald S, Trouton TG, O’Nunain SS, et al. *Circulation*. 1994;90:2501–2509.
13. Decreased defibrillator-induced dysfunction with biphasic rectangular waveforms. Jones JL, Jones RE. *Am J Physiol*. 1984;247:H792–H796.
14. Improved defibrillator waveform safety factor with biphasic waveforms. Jones JL, Jones RE, Balasky G. *Am J Physiol*. 1983;245:H60–H65.
15. Interruptions of Chest Compressions During Emergency Medical Systems Resuscitation. Terence D. Valenzuela, Karl B. Kern, Lani L. Clark, Robert A. Berg, Marc D. Berg, David D. Berg, Ronald W. Hilwig, Charles W. Otto, Daniel Newburn, Gordon A. Ewy. *Circulation*. 2005;112:1259-1265.

16. Tobacco Smoke Enemas. Ghislaine Lawrence. *The Lancet*. Volume 359, Issue 9315, Page 1442, 20 April 2002.
17. Safar P. History of cardiopulmonary-cerebral resuscitation, in Kay W and Bircher N, *Cardiopulmonary Resuscitation*, Churchill Livingstone, 1989, New York, pg 1-53.
18. *Swine in the Laboratory, Surgery, Anesthesia, Imaging, and Experimental Techniques*. Second Edition. M. Michael Swindle. 2007 Taylor & Francis Group. Boca Raton, FL. 33487-2742.
19. Why do chest compressions aid delayed defibrillation? Douglas Chamberlain, Michael Frenneaux, Stig Steen, Andrew Smith. *Resuscitation*. 2008;77:10-15.
20. The critical importance of minimal delay between chest compressions and subsequent defibrillation: a haemodynamic explanation. Stig Steen, Qiuming Liao, Leif Pierre, Audrius Paskevicius, Trygve Sjoberg. *Resuscitation*. 58 (2003) 249-258.
21. Coronary Perfusion Pressure and the Return of Spontaneous Circulation in Human Cardiopulmonary Resuscitation. Normon A. Paradis, Gerard B. Martin, Emanuel P. Rivers, Mark G. Goetting, Timoth J. Appleton, Marcia Feingold, Richard M. Nowak. *J Am Med Assoc*. 1990;263:8. 1106-1113.
22. Coronary perfusion pressure and the return of spontaneous circulation in human cardiopulmonary resuscitation. Paradis NA, Martin GB, Rivers EP, et al. *J Am Med Assoc*. 1990; 263:1106–1113.

23. Myocardial perfusion pressure: A predictor of 24-hour survival during prolonged cardiac arrest in dogs. Kern KB, Ewy GA, Voorhees WD, et al. *Resuscitation*. 1988; 16:241–250 .
24. Coronary perfusion pressure and return of spontaneous circulation after prolonged cardiac arrest. Reynolds JC, Salcido DD, Menegazzi JJ. *Prehosp Emerg Care*. 2010; 14:78–84.
25. Electrocardiogram waveforms for monitoring effectiveness of chest compression during cardiopulmonary resuscitation. Yongqin L, Ristagno G, Bisera J, et al. *Crit Care Med*. 2008; 36:211–215.
26. Expired PCO₂ as an index of coronary perfusion pressure. Sanders AB, Atlas M, Ewy GA, et al. *Am J Emerg Med*. 1985; 3:147–149.
27. Expired PCO₂ as a prognostic indicator of successful resuscitation from cardiac arrest. Sanders AB, Ewy GA, Bragg S, et al. *Ann Emerg Med*. 1985; 14:948–952.
28. Measurement of end-tidal carbon dioxide concentration during cardiopulmonary resuscitation. Steedman DJ, Robertson CE. *Arch Emerg Med*. 1990; 7:129–134.
29. End-tidal carbon dioxide monitoring during cardiopulmonary resuscitation: A prognostic indicator for survival. Sanders AB, Kern KB, Otto CW, et al. *J Am Med Assoc*. 1989; 262:1347–1351.
30. Partial pressure of end-tidal carbon dioxide successful predicts cardiopulmonary resuscitation in the field: A prospective observational study. Kolar M, Krizmaric M, Klemen P, et al. *Crit Care*. 2008; 12:R115.

31. Prediction of successful defibrillation in human victims of out of hospital cardiac arrest: A retrospective electrocardiographic analysis. Ristagno G, Gullo A, Berlot G, et al. *Anaesth Intensive Care*. 2008; 36:46–50.
32. Prediction of countershock success using single features from multiple ventricular fibrillation frequency bands and feature combinations using neural networks. Neurauter A, Eftestol T, Kramer-Johansen J, et al. *Resuscitation*. 2007; 73:253–263.
33. The predictive value of ventricular fibrillation electrocardiogram signal frequency and amplitude variables in patients with out of hospital cardiac arrest. Strohmenger H-U, Eftestol T, Sunde K, et al. *Anesth Analg*. 2001; 93:1428–1433.
34. Using within-patient correlation to improve the accuracy of shock outcome prediction for cardiac arrest. Gundersen K, Kvaloy JT, Kramer-Johansen J, et al. *Resuscitation*. 2008; 78:46–51.
35. Prediction of countershock success: A comparison of autoregressive and fast Fourier transformed spectral estimators. Nowak CN, Fischer G, Neurauter A, et al. *Methods Inf Med*. 2009; 48:486–492.
36. Predicting the success of defibrillation by electrocardiographic analysis. Povoas HP, Weil MH, Tang W, et al. *Resuscitation*. 2002; 53:77–82
37. Optimizing timing of ventricular defibrillation. Marn-Pernat A, Weil MH, Tang W, et al. *Crit Care Med*. 2001; 29:2360–2365.
38. Predictors of resuscitation outcome in a swine model of VF cardiac arrest: A comparison of VF duration, presence of acute myocardial infarction and VF

waveform. Indik JH, Shanmugasundaram M, Allen D, et al. *Resuscitation*. 2009; 80:1420–1423.

39. The influence of myocardial substrate on ventricular fibrillation waveform: A swine model of acute and postmyocardial infarction. Julia H. Indik, Richard L. Donnerstein, Ronald W. Hilwig, Matthias Zurcher, Justin Feigelman, Karl B. Kern, Marc D. Berg, Robert A. Berg. *Crit Care Med*. 2008 Vol 36, No.7; 2136-2142.
40. Methods for Calculating Coronary Perfusion Pressure During CPR. Michael P. Otlewski, Leslie A. Geddes, Michael Pargett, Charles F. Babbs; *Cardiovascular Engineering*. 9:98-103; 2009.